

Highly Selective and Solvent-Dependent Reduction of Nitrobenzene to N-Phenylhydroxylamine, Azoxybenzene and Aniline Catalyzed by Phosphino-Modified Polymer Immobilized Ionic Liquid-Stabilized AuNPs

Simon Doherty,^{*,†} Julian G. Knight,^{*,†} Tom Backhouse,[†] Ryan J. Summers,[†] Einas Abood,[†] William Simpson,[†] William Paget,[†] Richard A. Bourne,[‡] Thomas W. Chamberlain,^{‡,*} Rebecca Stones,[‡] Kevin R. J. Lovelock,[§] Jake M. Seymour,[§] Mark A. Isaacs,[¥] Christopher Hardacre,[†] Helen Daly,[†] and Nicholas H. Rees[†]

[†] NUCAT, School of Chemistry, Bedson Building, Newcastle University, Newcastle upon Tyne, NE1 7RU, UK

[‡] Institute of Process Research & Development, School of Chemistry and School of Chemical and Process Engineering, University of Leeds, Woodhouse Lane, Leeds, LS2 9JT, UK

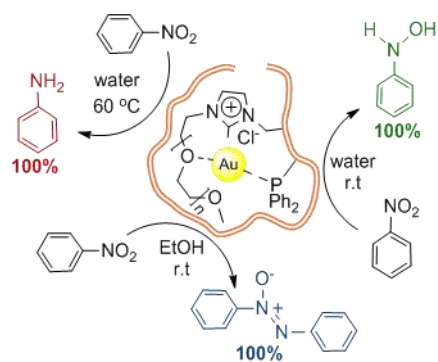
[§] School of Chemistry, Food and Pharmacy, University of Reading, Reading, RG6 6AT, UK

[¥] EPSRC National Facility for XPS (HarwellXPS), Room G.63, Research Complex at Harwell (RCaH), Rutherford Appleton Laboratory, Harwell, Oxford, Didcot, OX11 0FA, UK

[†] School of Chemical Engineering and Analytical Science, The Mill, Sackville Street Campus, The University of Manchester, Manchester M13 9PL, UK

[‡] Inorganic Chemistry Laboratory, University of Oxford, South Parks Road, Oxford OX1 3QR

Table of Contents and Abstract Graphics



ABSTRACT: Gold nanoparticles stabilized by phosphine-decorated polymer immobilized ionic liquids (AuNP@PPh₂-PIILP) is an extremely efficient multi-product selective catalyst for the sodium borohydride-mediated reduction of nitrobenzene giving either *N*-phenylhydroxylamine, azoxybenzene or aniline as the sole product under mild conditions and a very low catalyst loading. The use of a single nanoparticle-based catalyst for the partial and complete reduction of nitroarenes to afford three different products with exceptionally high selectivities is unprecedented. Under optimum conditions, thermodynamically unfavorable *N*-phenylhydroxylamine can be obtained as the sole product in near quantitative yield in water whereas a change in reaction solvent to ethanol results in a dramatic switch in selectivity to afford azoxybenzene. The key to obtaining such a high selectivity for *N*-phenylhydroxylamine is the use of a nitrogen atmosphere at room temperature as reactions conducted under an inert atmosphere occur via the direct pathway and are essentially irreversible while reactions in air afford significant amounts of azoxy-based products by virtue of competing condensation due to reversible formation of *N*-phenylhydroxylamine. Ultimately, aniline can also be obtained quantitatively and selectively by adjusting the reaction temperature and time accordingly. Introduction of PEG onto to the polyionic liquid resulted in a dramatic improvement in catalyst efficiency such that *N*-phenylhydroxylamine could be obtained with a TON of 100,000 (TOF of 73,000 h⁻¹, with >99% selectivity), azoxybenzene with a TON of 55,000 (TOF of 37,000 h⁻¹ with 100% selectivity) and aniline with a TON of 500,000 (TOF of 62,500 h⁻¹, with 100% selectivity). As the combination of ionic liquid and phosphine are required to achieve high activity and selectivity further studies are currently underway to explore whether interfacial electronic effects influence adsorption and thereby selectivity and whether channeling of the substrate by the electrostatic potential around the AuNPs is responsible for the high activity. This is the first report of a AuNP-based system that can selectively reduce nitroarenes to either of two

synthetically important intermediates as well as aniline and, in this regard, is an exciting discovery that will form the basis to develop a continuous flow process enabling facile scale-up.

KEYWORDS: *Nanoparticle catalysis, gold, selective partial reduction, nitroarenes, N-phenylhydroxylamine, azoxybenzene, aniline, switchable selectivity*

INTRODUCTION

Selectivity in catalysis is immensely important for the industrial scale production of commodity chemicals as well as fine chemicals and pharmaceuticals as it limits the production of waste, streamlines the process by avoiding or simplifying purification procedures, reduces costs and improves green credentials.¹ While selectivity in homogeneous catalysis is well-understood and can often be optimized by tuning steric and electronic parameters,² tuning selectivity of nanoparticles or heterogeneous catalysts is much more challenging and less-well developed.³ To this end, until recently, the vast majority of studies have employed organic modifiers which improve or enhance selectivity through steric effects resulting from specific noncovalent molecular interactions.⁴ However, there is now a growing body of evidence that activity and selectivity of nanoparticle-based catalysts can be modified/optimized by modulating their surface electronic structure. For example, PVP-stabilized rhodium nanoparticles modified with phosphine catalyze the chemoselective hydrogenation of functionalized aromatic compounds with >92% selectivity compared with 70% for the unmodified catalyst⁵ while addition of tricyclohexylphosphine to silica-supported CuNPs results in a significant improvement for the semi-hydrogenation of 1-phenyl-1-propyne to *cis*- β -methylstyrene.⁶ Other relevant studies include gold nanoparticles ligated by secondary phosphine oxides which catalyze the hydrogenation of α,β -unsaturated aldehydes with 100% selectivity for reduction of the carbonyl⁷ and a pronounced ligand effect for RhNP and RuNP catalyzed hydrogenation of aromatic ketones⁸ and substituted arenes.⁹ Most recently, platinum nanoparticles stabilized on triphenylphosphine-modified silica showed markedly higher selectivity for the chemoselective hydrogenation of acetophenone and phenylacetylene than its unmodified counterpart; this too has been attributed to an increase in surface electron density by the electron donating phosphine.¹⁰ In addition, amine-based modifiers

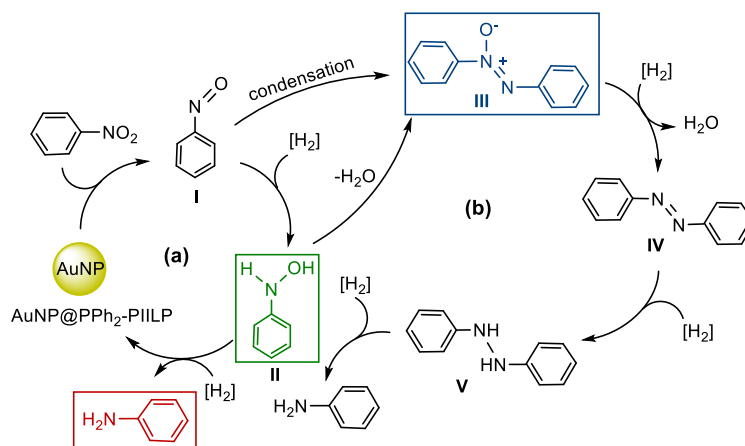
have also been shown to alter the surface electronic structure of platinum nanowires and particles and thereby optimize reaction selectivity for the partial hydrogenation of nitroarenes to N-arylhydroxylamines.¹¹ The high activity of amino-modified Ru/ γ -Al₂O₃ for the aqueous phase hydrogenation of levulinic acid to γ -valerolactone was attributed to highly dispersed ruthenium centers with an electron-rich state¹² and the efficacy of RuNP stabilized in amine-modified porous organic polymers for the catalytic transfer hydrogenation of nitroarenes was attributed to a combination of nano-confinement and electron donation¹³ while the efficacy of PdNPs supported on amine-rich silica hollow nanospheres for the hydrogenation of quinoline has been associated with an ultra-small particle size and high surface electron density.¹⁴ Amine modified supports have been shown to improve activity and selectivity for PtNP, Pt/Co-NP and PdNP-catalyzed semi-hydrogenation of alkynes^{15a-c} and selectivity for PtNP-catalyzed reduction of the C=O double bond in cinnamaldehyde^{15d} while functionalization of platinum nanoparticles with *L*-proline enhances the activity and selectivity for the hydrogenation of acetophenone.¹⁶ Aspartic acid also improves the activity and selectivity of platinum nanoparticle catalysts for the selective hydrogenation of α,β -unsaturated aldehydes to unsaturated alcohols through cooperation of steric and electronic effects.¹⁷ Finally, a series of elegant studies by the Glorious group have also demonstrated that the performance of supported heterogeneous catalysts can be tuned by surface modification with N-heterocyclic carbenes which activate unreactive Pd/Al₂O₃ for the Buchwald-Hartwig amination,¹⁸ improve the selectivity of Ru/K-Al₂O₃ for the hydrogenation of aryl ketones and alkynes¹⁹ and influence the performance and stability of ruthenium and palladium nanoparticles as catalysts for oxidations and reductions.²⁰

We have recently been exploring the concept of HeteroAtom Donor-modified Polymer-Immobilized Ionic Liquid Stabilized NPs (NP@HAD-PIILS) reasoning that covalent attachment

of an ionic liquid to a polymer would combine the favorable characteristics of ILs, such as their tunable physicochemical properties, ease of modification and enhancement in reaction rates and selectivity with the advantages associated with attachment to a solid support, to limit loss of ionic liquid, facilitate product separation, catalyst recovery and recycle and reduce the volume of IL as the catalyst is retained in a small amount of PIIL.²¹ While heteroatom donors were initially incorporated into ionic liquids to stabilize NPs with respect to agglomeration under conditions of catalysis,²² it is now clear that these donors could also enable the surface electronic structure to be modified and/or NP size and morphology to be controlled and, in this regard, HAD-PIILs may well prove to be tunable multifunctional supports for developing more efficient catalysts and processes.^{14c,7a,15a,15d,22p} Gratifyingly, our initial foray in this area has proven extremely promising as PEG-modified phosphine-decorated polymer-immobilized ionic liquid-stabilized palladium nanoparticles were shown to be remarkably active and selective catalysts for hydrogenation of α,β -unsaturated aldehydes, ketones and nitriles,²³ hydrogenation and transfer hydrogenation of nitroarenes in water²⁴ and Suzuki-Miyaura cross-couplings in aqueous media.²⁵

With the aim of further exploring the concept of PIIL stabilized NPs we have recently extended our study to include gold nanoparticle-based systems in order to undertake a comparative study of their efficacy as catalysts for the reduction of nitroarenes. Herein, we report that AuNP@PPh₂-PIILP and its PEGylated counterpart AuNP@PPh₂-PEGPIILP are highly efficient and remarkably selective catalysts for the sodium borohydride-mediated reduction of nitroarenes to either *N*-phenylhydroxylamine, azoxybenzene or aniline (Scheme 1). Although AuNP catalyzed reduction of nitroarenes with sodium borohydride have been widely reported in the literature,²⁶ the overwhelming majority of systems are highly selective for aniline and this is the first example of a AuNP-based catalyst that is completely selective for the aqueous phase sodium borohydride-

mediated reduction of a nitroarene to either the corresponding *N*-arylhydroxylamine, azoxyarene or aniline. To this end, there are very few reports of a single catalyst that can selectively reduce a nitroarene to more than one intermediate with high efficacy. For example, RuNPs catalyze the transfer hydrogenation of nitroarenes to the corresponding azoxyarene, azoarene or aniline, albeit with moderate selectivities and at elevated temperatures with a high catalyst loading.^{27a} More recently, Au/meso-CeO₂ has been shown to be a highly selective and switchable catalyst for the transfer hydrogenation of nitroarenes to the corresponding azoxyarene, azoarene or aniline and high yields of each product could be obtained by modifying the reaction conditions.^{27b}



Scheme 1 General mechanisms (Haber) for the reduction of nitroarenes (a) direct pathway (b) condensation pathway, highlighting the selective partial reduction to *N*-phenylhydroxylamine (green), azoxybenzene (blue) and complete reduction to aniline (red) achieved with AuNP@PPh₂-PIILP (**3a**) and AuNP@PPh₂-PEGPIILP (**3a.PEG**).

Selective partial hydrogenation of nitroarenes is of considerable interest as *N*-arylhydroxylamines are synthetically important intermediates to high value products including biologically active motifs,²⁸ polymerization inhibitors²⁹ and reagents for use in organic synthesis as they undergo a range of transformations including cyclizations,^{30a} the Bamberger

rearrangement^{30b} and gold-catalyzed additions to multiple bonds.^{30c} Although there are numerous procedures for the synthesis of *N*-arylhydroxylamines including stoichiometric reductions with zinc or tin³¹ as well as catalytic reductions using Rh/C,^{32a,b} Pt/SiO₂,^{32c} RuNP/carbon nanotubes,^{32d} RuNP/polystyrene,^{32e} and PtNP/Amberlite IRA^{32f} all with hydrazine, AgNP/TiO₂ with ammonia-borane^{32g} and ultra-thin PtNW/amine,^{11a} PtNP/amine,^{11b} Pt/SiO₂-amine,^{33a} Pt/C-DMSO^{33b} and platinum metal catalysts^{33c} with hydrogen, most suffer severe limitations including low isolated yields, poor selectivity, slow rates, a lack of scalability and/or recyclability as well as poor environmental and economical credentials. Similarly, azoxyarenes are an important class of compound which find use as dyes, reducing agents and chemical stabilizers.³⁴ Azoxyarenes have been prepared by stoichiometric³⁵ or catalytic^{34,36} oxidative coupling of arylamines as well as selective reduction of nitroarenes,^{27,37} however, these approaches also suffer the same drawbacks as those detailed above for the selective synthesis of *N*-arylhydroxylamines. As such, the discovery of a single catalyst that is highly selective for the reduction of nitroarenes to *N*-arylhydroxylamines, azoxyarenes and the corresponding aniline at low catalyst loadings in either water or ethanol under mild conditions is exceptional and will provide a platform to engineer new catalyst technology for efficient cost-effective production of these target intermediates.

EXPERIMENTAL SECTION

Synthesis of Catalyst Precursor [AuCl₄]Cl@PPh₂-PIILP (2a). A 100 mL round bottom flask was charged with the appropriate PPh₂-PIILP (1.79 g, 2.0 mmol) support and water (15 mL). To this was added a solution of potassium tetrachloroaurate (0.755 g, 2.0 mmol) in water (4-5 mL) and the resulting mixture stirred vigorously for 6 hours. The yellow precipitate was collected after centrifugation by filtration through a frit and the solid was washed with water (10 mL), ethanol (2

x 10 mL) and diethyl ether (3 x 10 mL) to afford the corresponding afford the desired precatalyst **2a** as a pale-yellow powder in 93% yield (2.2 g). ICP-OES data: 0.73 wt% gold and a gold loading of 0.037 mmol g⁻¹.

Synthesis of [AuCl₄]Br@PPh₂-PEGPIILP (2a.PEG). Tetrachloroaurate loaded polymer **2a.PEG** was prepared according to the procedure described above for **2a** and isolated as a pale-yellow powder in 87% yield. ICP-OES data: 3.1 wt% gold and a gold loading of 0.16 mmol g⁻¹.

General procedure for the selective reduction of nitroarenes to arylhydroxylamines. A Schlenk flask equipped with a magnetic stirrer was charged with precatalyst (0.5 μmol, 0.005 mol % gold based on the gold loading determined as mmol Au g⁻¹ polymer using ICP-OES data) and evacuated and backfilled with nitrogen. NaBH₄ (0.096 g, 2.5 mmol) was added followed immediately by water (2.5 mL) and the resulting mixture stirred vigorously for 5 min at room temperature. After this time, nitroarene (1 mmol) was added and the reaction stirred for the appropriate time. The reaction was quenched by addition of ethyl acetate (20 mL) followed by water (5 mL), the organic phase separated after extractions and the solvent removed under reduced pressure. The residue was analyzed by ¹H NMR spectroscopy using 1,4-dioxane as internal standard to quantify the composition of starting material and products and determine the selectivity.

General procedure for the selective reduction of nitrobenzene to azoxybenzene. A Schlenk flash was charged with precatalyst (0.5 μmol, 0.005 mol % gold based on the gold loading determined as mmol Au g⁻¹ polymer using ICP-OES data) under a nitrogen atmosphere and NaBH₄ (0.096 g, 2.5 mmol) and ethanol (2 mL) added. The solution was stirred for 5 mins at room temperature after which time nitrobenzene (102 μL, 1 mmol) was added and the resulting mixture stirred for the appropriate time. After this, stirring was stopped, 1,4 dioxane (85 μL, 1 mmol) was

added as the internal reference and an aliquot (*ca.* 0.05 mL) removed and diluted with CDCl₃ (0.35 mL). The reaction was analyzed using ¹H NMR spectroscopy to quantify the composition and selectivity.

General procedure for the reduction of nitroarenes to arylamines. A Schlenk flask was charged with precatalyst (0.5 μmol, 0.005 mol % gold based on the gold loading determined as mmol Au g⁻¹ polymer using ICP-OES data) under a nitrogen atmosphere and NaBH₄ (0.192 g, 5.0 mmol) and water (2 mL) added. The solution was then stirred for 5 mins at room temperature after which nitrobenzene (102 μL, 1 mmol) was added dropwise and the mixture heated to 60°C with stirring for the appropriate time. After this time, the reaction was cooled to room temperature then quenched by addition of ethyl acetate (40 mL) and water (5 mL), the aqueous phase separated after extraction and the solvent removed under reduced pressure. The residue was analyzed by ¹H NMR spectroscopy using 1,4-dioxane as internal standard to quantify the composition and selectivity.

RESULTS AND DISCUSSION

Synthesis and characterization of phosphine-modified gold precatalysts and nanoparticles

The polymers, their tetrachloroaurate loaded precursors, and the corresponding polymer immobilized ionic liquid stabilized AuNPs developed in this project are shown in Figure 1. These polymers have been designed to form a protective cage or shell over the AuNP surface that provides stabilization through electrostatic interactions with the imidazolium fragment as well as Au-P interactions with the phosphine-decorated polymer.³⁸ Polymer immobilized ionic liquids **1a** and **1b** were prepared by AIBN-initiated radical polymerization of the constituent imidazolium-modified monomer or its PEGylated counterpart with cation appropriate cross-linker and 4-diphenylphosphinostyrene in the desired ratio.²³⁻²⁵ Both polymers were impregnated by

exchanging half of the halide anions with $[\text{AuCl}_4]^-$ to afford the corresponding tetrachloroaurate-loaded precursors **2a** ($[\text{AuCl}_4]\text{Cl}@P\text{Ph}_2\text{-PIILP}$) and **2a.PEG** ($[\text{AuCl}_4]\text{Br}@P\text{Ph}_2\text{-PEGPIILP}$) which have a gold to phosphine stoichiometry of one; full characterization details are provided in the ESI. As we have previously demonstrated that palladium nanoparticle-based catalysts generated *in situ* by reduction of the corresponding tetrachloropalladate-loaded precursor immediately prior to use are as efficient as their *ex situ* prepared counterparts, precursors,²⁴⁻²⁵ **2a** and **2a.PEG** were used for catalyst evaluation and optimization while samples of **3a** and **3a.PEG** were generated under conditions of catalysis to obtain TEM and XPS characterization data on the active species. The generation of catalyst *in situ* immediately prior to addition of substrate offers several potential practical advantages as it eliminates the need to prepare, isolate and store nanoparticle catalysts, and as such streamlines the protocol; it also improves versatility by enabling different reducing agents and/or conditions to be examined and thereby facilitates rapid catalyst and reaction screening.

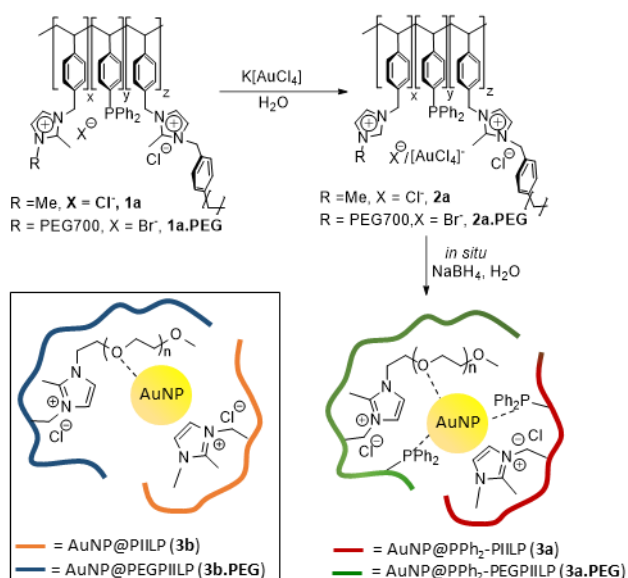


Figure 1 Composition of polymers **1a** and **1a.PEG**, synthesis of $[\text{AuCl}_4]^-$ impregnated polymers **2a** and **2a.PEG** and PIILP-stabilized gold nanoparticles **3a** (red) and **3a.PEG** (green) and composition of **3b** (orange) and **3b.PEG** (blue).

The gold loadings of precatalysts **2a** and **2a.PEG** were determined to be $0.037 \text{ mmol g}^{-1}$ and 0.16 mmol g^{-1} , respectively, using ICP-OES. The solid state ^{31}P NMR spectra of **2a** and **2a.PEG** confirm the presence of a Au---P interaction which is clearly evident from the low field chemical shifts of $\delta 27.1$ and 24.5 ppm, respectively; for comparison the ^{31}P NMR signals for polymers **1a** and **1a.PEG** appear at $\delta -5$ and -10.4 ppm, respectively (see ESI file for full details); these complexation shifts³⁹ are similar to previously reported values.⁴⁰ The ^{13}C CP/MAS NMR spectra of **1a** and **1a.PEG** and **2a** and **2a.PEG** contain a set of characteristic signals between $\delta 124$ - 144 ppm associated with the imidazolium ring and the aromatic carbon atoms as well as signals in the range $\delta 11$ - 50 ppm which correspond to the methyl groups attached to the imidazolium ring and the aliphatic carbon atoms of the polystyrene backbone (see ESI file for full details). ATR-IR spectra of catalysts **2a** and **2b**, treated *in-situ* with NaBH_4 /ethanol solution to form AuNP, showed no adsorption of CO due to weak adsorption of CO on metallic Au. Surface characterization of the tetrachloroaurate-loaded precursors (**2a**, **2b**, **2a.PEG** and **2b.PEG**) and equivalent reduced catalysts (**3a**, **3b**, **3a.PEG** and **3b.PEG**) was undertaken by X-ray photoelectron spectroscopy (XPS) and a shift in the Au $4f_{5/2}$ and Au $4f_{7/2}$ doublets to lower binding energies upon reduction was observed (see ESI file for details). For example, Au $4f_{7/2}$ binding energies of 87.4 eV for **2b** and 87.6 eV for **2b.PEG** are entirely consistent with the Au^{3+} ion^{41a,b} whilst 83.8 eV for **3b** and 83.8 eV for **3b.PEG** are assigned to a lower oxidation state of the Au species (Au^0) (Figure 2a-b).^{41b,c} For example, the Au $4f_{7/2}$ binding energies are similar to those found for AuNPs supported

on IL-hybrid γ -Al₂O₃ materials in which the ionic liquid moiety forms a thin layer that acts as a cage for the AuNPs.^{41d} The presence of additional Au 4f doublets in the precursor spectra at higher binding energies than the Au⁰ doublets of the chemically reduced catalysts are assigned as Au¹ species resulting from decomposition caused by exposure to the X-ray source during acquisition,^{41e} this is particularly evident in the spectra for **2a** in which the sample has undergone near complete reduction. This is verified by considering the N 1s region, which along with the expected signal for the imidazolium environment in each sample, shows additional signals at lower binding energies corresponding to uncharged, and in some cases anionic, nitrogen species which are assigned to damage.^{41f} There is no evidence from the XPS of any Au---P interactions caused by electron donation from the phosphino group, identified by solid state NMR spectroscopy as the binding energies for the Au 4f_{5/2} and Au 4f_{7/2} doublets for both **2a** and **2a.PEG** are very similar to those of **2b** and **2b.PEG** (Figure 2b and ESI); moreover, no shift in the binding energies of the P 2p_{3/2} and P 2p_{1/2} doublets was observed upon reduction of the gold salt (Figure 2c).

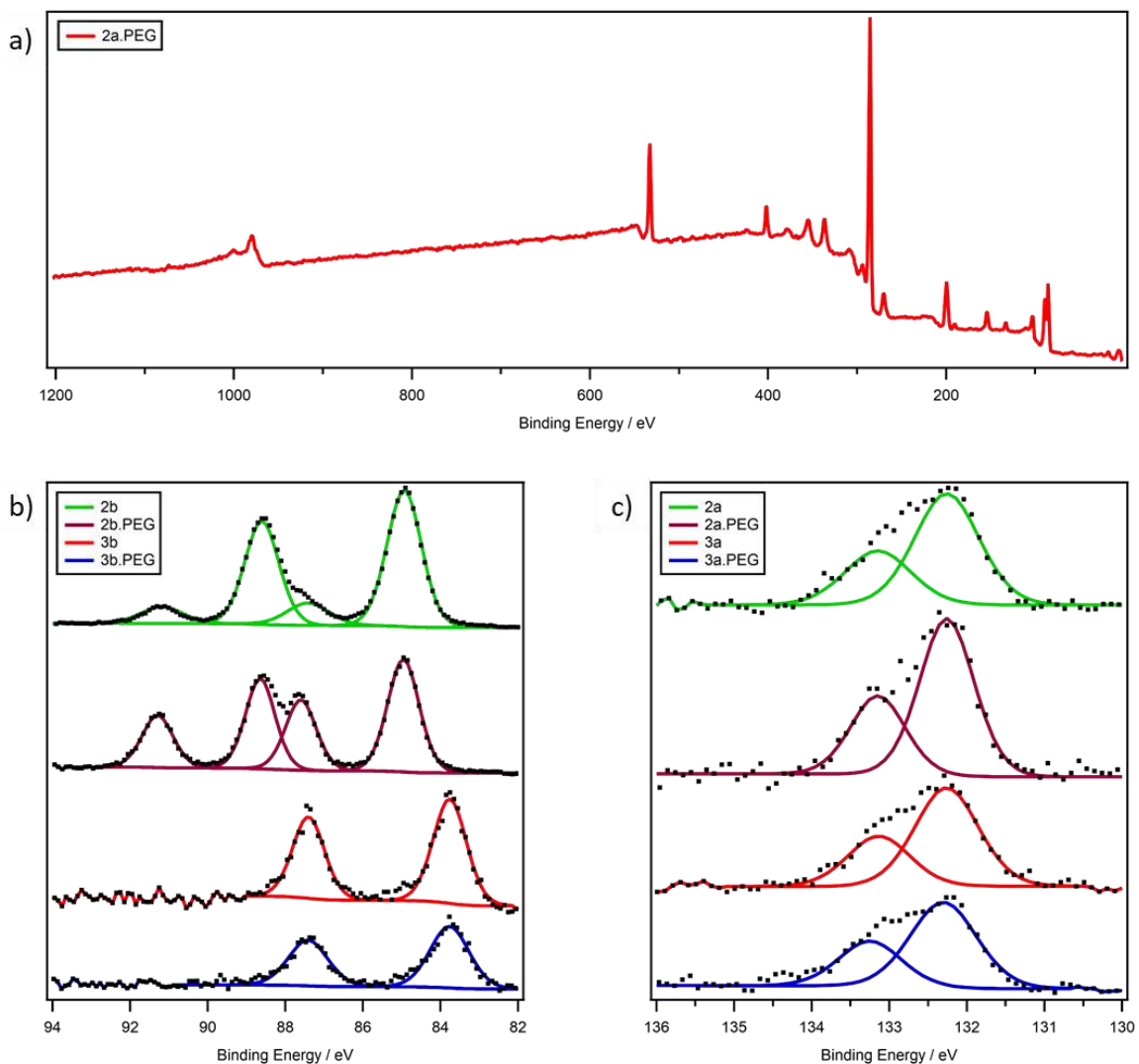


Figure 2 XPS scan showing a) full scan of **2a.PEG**; b) Au 4f core level of **2b**, **2b.PEG** and **3b** and **3b.PEG**; and (c) P 2p core level of **2a**, **2a.PEG** and **3a** and **3a.PEG**. All referenced to the C 1s alkyl peak at 284.8 eV.

TEM micrographs of *in situ* generated **3a** and **3a.PEG** revealed that the gold nanoparticles were near monodisperse with average diameters of 3.4 ± 0.9 and 2.5 ± 0.6 nm, respectively, representative micrographs and associated distribution histograms based on > 100 particles are shown in Figure 3 (see ESI file for TEM micrographs of **3b** and **3b.PEG**). For comparison, AuNPs

supported on IL-hybrid γ -Al₂O₃ have slightly larger mean diameters of 6.5-6.7 nm, however, these systems were prepared by sputtering deposition using ultrapure gold foil whereas **3a** and **3a.PEG** were prepared by reduction of a gold(III) salt.^{41d} Interestingly, we have recently reported that palladium nanoparticles stabilized by PPh₂-PIILP and PPh₂-PEGPIILP have vastly disparate sizes and those stabilized by polymer immobilized ionic liquid containing PEG and PPh₂ were also smaller than those stabilized by PPh₂-modified PIIL; thus, the number and type of heteroatom donor may well influence nucleation and growth of NPs. The strong surface plasmon resonance (SPR) adsorption for AuNPs is dependent on the size and shape as well as the dielectric constant of the local medium which for this study will be associated with the nature of the polymeric shell.^{38,42,43} The strong SPR bands at 519 nm in the UV-vis spectra of AuNP@PPh₂-PIILP (**3a**) and AuNP@PPh₂-PEGPIILP (**3a.PEG**) and at 517 nm for AuNP@PEG-PIILP (**3b.PEG**) are consistent with formation of spherical particles while λ_{max} for AuNP@PIILP (**3b**) is red shifted to 525 nm, which may well reflect the different nature of the ligand-surface interactions stabilizing the NPs as the ionic microenvironment in each is approximately the same but **3b** is the only system that does not contain heteroatom donor atoms. As a comparison, gold nanoparticles stabilized by neutral PEG-modified heteroatom donor mono- bis- and tris-1,2,3-triazoles as well as nona-PEG-branched triazole dendrimers with diameters close to 3 nm also exhibit SPR bands around 515 nm.^{26d-f}

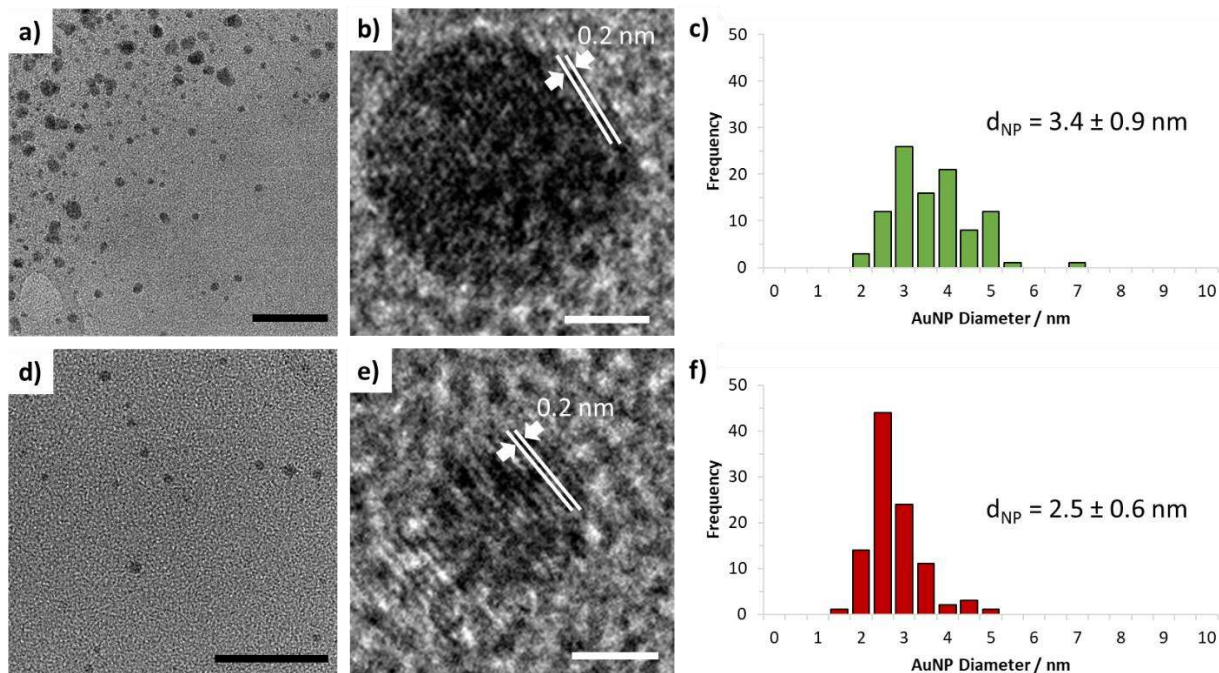


Figure 3 HRTEM images of (a-b) **3a** and (d-e) **3a-PEG**, with the observed atomic spacing (parallel white lines) confirming the metallic nature of the AuNPs, and (c and f) corresponding particle size distributions determined by counting >100 particles. Mean nanoparticle diameters are of 3.4 ± 0.9 nm and 2.5 ± 0.6 nm for **3a** and **3a-PEG**, respectively. Black and white scale bars are 25 and 1 nm, respectively.

Selective Reduction of Nitrobenzene to *N*-Phenylhydroxylamine

The reduction of nitroarenes was initially targeted on the basis that there have been two recent reports that nitrogen donor-modified platinum nanoparticles selectively catalyze the highly selective partial hydrogenation of nitrobenzene to *N*-phenylhydroxylamine.¹¹ As the high selectivity of these systems was attributed to electron donation from the amine to the surface platinum atoms, we became interested in exploring and comparing the efficacy of phosphine-decorated PIII-stabilized AuNPs as catalysts for the reduction of nitroarenes to assess the

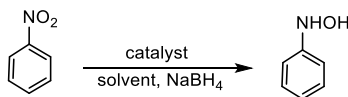
influence of the heteroatom donor on selectivity; moreover, embedding the selectivity modifying heteroatom donor in to the support will eliminate the need to separate or recover the additive which will simplify work-up and facilitate recycling. To this end, we have recently demonstrated that PdNP@PIILP are highly efficient catalysts for the complete reduction of nitroarenes to the corresponding aniline in water under extremely mild conditions and the TOF of 17,125 h⁻¹ is the highest to be reported for the aqueous phase transfer hydrogenation of a nitroarene catalyzed by a PdNP-based system.²⁴

A series of catalytic reactions were initially conducted with nitrobenzene as the benchmark substrate using a protocol recently developed for the PdNP-catalyzed reduction of nitroarenes as a lead.²⁴ A preliminary reaction conducted in water under air for 40 min at 25 °C using a 0.005 mol% loading of AuNP@PPh₂-PIILP (**3a**), generated *in situ* by reduction of tetrachloroaurate loaded **2a**, with a substrate:NaBH₄ ratio of 2.5 gave 35% conversion and 62% selectivity for *N*-phenylhydroxylamine (Table 1 entry 1). Under these conditions, azoxybenzene was identified as the other major species (10%) together with trace amounts of azobenzene (2%) and aniline (2%). An increase in the reaction time to 6 h resulted in complete conversion affording a complex mixture containing azoxybenzene (41%), *N*-phenylhydroxylamine (36%) and azobenzene (20%) as the major components together with a minor amount of diphenylhydrazine (<1%) and aniline (2%); this product distribution is consistent with reduction *via* the condensation pathway (Table 1 entry 2). Speculating that reversible reduction of rapidly formed nitrosobenzene to *N*-phenylhydroxylamine in air would facilitate access to the condensation pathway to afford azoxy-based reduction products, the same reaction was conducted under a nitrogen atmosphere. Remarkably, the same reaction conducted under a nitrogen atmosphere for 40 min resulted in a

dramatic improvement in selectivity from 62% to 97% as well as an increase in conversion to 45%; moreover, high selectivity for *N*-phenylhydroxylamine was retained when the reaction time was extended to 6 h (Table 1 entries 3 and 4), which is in stark contrast to the corresponding reaction conducted in air (Table 1 entries 1 and 2). Thus, it appears that irreversible formation of *N*-phenylhydroxylamine under nitrogen suppresses the condensation pathway as only trace quantities of azoxybenzene (1%) and aniline (<1%) were detected by NMR spectroscopy and GLC analyses. Indeed, we are confident that azoxybenzene only forms after exposure of the sample to oxygen during work-up, as monitoring of the NMR sample showed a significant increase in azoxybenzene with time at the expense of *N*-phenylhydroxylamine; as such all subsequent studies were conducted with careful and meticulous exclusion of air. A survey of the performance of **3a** in selected solvents revealed that the highest conversions and selectivities were obtained in water whereas markedly lower yields and/or selectivities were obtained under the same conditions in ethanol, a 1:1 mixture of ethanol and water, 2-methyltetrahydrofuran, a 1:1 mixture of water and 2-methyltetrahydrofuran and toluene (Table 1 entries 3-9). Most interestingly, this study revealed that the use of ethanol as solvent gave a complete switch in selectivity to afford azoxybenzene as the sole product albeit with a conversion of only 19% (Table 1 entry 5); full details are discussed in the following section on selective reduction of nitrobenzene to azoxybenzene and aniline. To this end, AuNPs supported on *meso*-CeO₂ catalyze the sodium borohydride-mediated transfer hydrogenation of nitroarenes with solvent-dependent switchable selectivity to afford azoxyarene as the sole product in 2-propanol and the azoarene in a mixture of 2-propanol and water.^{27b}

Thus, water was identified as the solvent of choice based on the high conversion and superior and unprecedented selectivity for *N*-phenylhydroxylamine as well as its environmentally benign properties, practical advantages and the potential benefit of the hydrophobic effect.

Table 1 Selective reduction of nitrobenzene to *N*-phenylhydroxylamine by NaBH₄ as a function of catalyst, solvent and temperature.^a



entry	Catalyst	Solvent	Temp (°C)	Mol% cat	Time (min)	Conv (%) ^b	Select (%) ^c
1	3a^d	water	25	0.005	40	35	62
2	3a^d	water	25	0.005	360	100	41
3	3a^e	water	25	0.005	40	45	97
4	3a^e	water	25	0.005	360	100	96
5	3a^{e,f}	EtOH	25	0.005	40	19	0
6	3a^e	EtOH/water	25	0.005	40	34	92
7	3a^e	2-MeTHF	25	0.005	40	1	>99
8	3a^e	2-MeTHF/water	25	0.005	40	17	98
9	3a^e	toluene	25	0.005	40	2	>99
11	3a^e	water	25	0.025	40	81	92
12	3a^e	water	50	0.005	40	100	83
13	3a.PEG^e	water	25	0.005	40	100	>99
14	AuNP@citrate^e	water	25	0.005	40	22	87
15	3b^e	water	25	0.005	40	27	97
16	3b.PEG^e	water	25	0.005	40	55	96

^a Reaction conditions: 1 mmol nitrobenzene, mol% Au in **3a**, **3a.PEG**, **3b**, **3b.PEG** and AuNP@citrate, 2 mL solvent, 2.5 mmol NaBH₄, time, temperature. ^b Yields determined by ¹H NMR spectroscopy using dioxane as internal standard and gas chromatography using decane as internal standard. Average of at least three runs. ^c Selectivity for *N*-phenylhydroxylamine [%*N*-phenylhydroxylamine / (% *N*-phenylhydroxylamine + % azoxybenzene + % azobenzene + % aniline)] / x 100%. ^d Reaction conducted in air. ^e Reaction conducted under N₂. ^f Reaction in ethanol gave 19% conversion with 100% selectivity for azoxybenzene.

Variation of the catalyst loading revealed that the optimum combination of conversion and selectivity was obtained with 0.005 mol% **3a** as a loading of 0.025 mol% resulted in a slight drop in selectivity due to formation of aniline (Table 1 entry 10). As a large excess of sodium borohydride is often employed for the reduction of nitroarenes, the NaBH₄ to substrate ratio was varied and conversions were shown to increase quite dramatically from 9% with 1.0 equivalent eventually reaching a plateau of 71% with 15 equivalents (Figure 4). While this profile is a clear indication of mass transfer limited availability of reducing agent, the TOFs will still be limited by the poor solubility of the substrate in water even with an excess of borohydride. As such, all further studies were conducted using 2.5 equivalents of NaBH₄ as this was the best compromise giving good conversions after a relatively short reaction time (2 h); the use of only a slight excess of reducing agent also improves the overall atom efficiency.

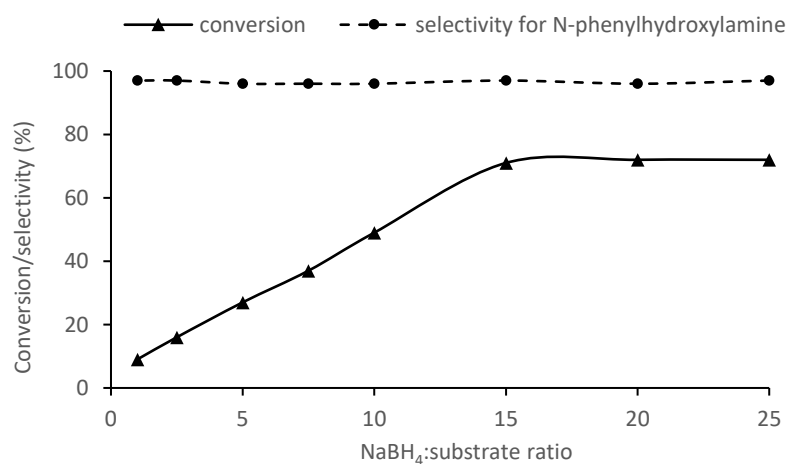


Figure 4 Reaction profile (conversion and selectivity for *N*-phenylhydroxylamine) as a function of the NaBH₄:substrate ratio for the reduction of nitrobenzene in water under nitrogen at 25 °C catalyzed by 0.005 mol% **3a** for a reaction time of 30 min.

Selectivity for *N*-phenylhydroxylamine decreased with an increase in the reaction temperature due to the formation of increasing amounts of aniline; for example, *N*-phenylhydroxylamine was obtained in 83% yield and selectivity together with 14% aniline and 3% azoxybenzene after 2 h at 50 °C (Table 1 entry 12) while a further increase in the reaction temperature to 80 °C gave 27% aniline and 71% *N*-phenylhydroxylamine. The nature of this temperature-dependent selectivity suggests that the activation barrier for reduction of *N*-phenylhydroxylamine to aniline with catalyst **3a** may be higher than that for reduction of nitrobenzene (or nitrosobenzene) to *N*-phenylhydroxylamine; this would allow high selectivities to be obtained for reactions conducted at lower temperatures. To this end, Vogt recently reported a similar temperature-dependent selectivity for the hydrogenation of nitrobenzene catalyzed by supported PtNPs as the formation of *N*-phenylhydroxylamine was favored over aniline at reaction temperatures below 30 °C while above 60 °C *N*-phenylhydroxylamine and aniline formed at similar rates such that selectivity for the former dropped to 18% at 100 °C.^{11b} However, even though the activation barrier for reduction of *N*-phenylhydroxylamine to aniline is clearly high enough to obtain *N*-phenylhydroxylamine with high selectivity (96% at complete conversion after 2 h at 25 °C) it is also possible to obtain aniline as the sole product by increasing the reaction time and/or temperature accordingly (see later). Further kinetic studies will be required to elucidate the relative rate of *N*-phenylhydroxylamine formation compared with *N*-phenylhydroxylamine reduction. A control reaction for the reduction of nitrobenzene conducted at room temperature in water under nitrogen using 2.5 equivalents of NaBH₄ but in the absence of **3a** gave no conversions even after 3 h.

As the high selectivity of **3a** for *N*-phenylhydroxylamine was obtained in water the influence of introducing PEG on to the polymer immobilized ionic liquid was examined reasoning that an increase in hydrophilicity would improve water solubility and/or catalyst dispersibility and thereby

efficiency while additional interactions between the oxygen donors of the ether and surface atoms of the nanoparticle could provide further stabilization. Under the same conditions identified above, 0.005 mol% **3a.PEG** catalyzed the reduction of nitrobenzene to give complete conversion with 99% selectivity for *N*-phenylhydroxylamine after a reaction time of only 40 min (Table 1 entry 13); this is a significant improvement on the efficacy of **3a** which required 2 h to reach 100% conversion (Table 1 entry 4). A comparative study of the variation in composition as a function of time for the reduction of nitrobenzene catalyzed by **3a** and **3a.PEG** at 25 °C (Figure 5) clearly shows the disparate rates of formation of *N*-phenylhydroxylamine which we tentatively attribute to the hydrophilicity of the PEGylated support facilitating access of the substrate to the active site. While the different size distributions of **3a** (3.4 ± 0.9 nm) and **3a.PEG** (2.5 ± 0.6 nm) may well also be activity determining, we note that **3b** (3.4 ± 1.1 nm) and **3b.PEG** (3.3 ± 0.9 nm) have similar mean diameters but the latter is markedly more active, as evidenced by the disparate conversions obtained after 40 min (Table 1 entries 15 and 16), which is a strong indication that the PEGylated support contributes to the improvement in activity. While AuNPs stabilized by an amphiphilic PEG-modified tris-triazole has recently been reported to be a highly active catalyst for the sodium borohydride-mediated reduction of 4-nitrophenol, in stark contrast to **3a.PEG** this system gave complete reduction to 4-aminophenol.^{26g} The high selectivity of **3a-PEG** as a catalyst for the reduction of nitrobenzene to *N*-phenylhydroxylamine is clearly evident from a comparison of the ¹H NMR spectrum of a typical reaction mixture obtained after only 30 min (Figure 6b) with that of nitrobenzene (Figure 6a). As there are no reports of selective partial reduction of nitroarenes to *N*-phenylhydroxylamine with gold-based nanoparticles, benchmark comparative catalyst testing was undertaken using a 0.005 mol% loading of AuNP@citrate generated *in situ* by reduction of potassium tetrachloroaurate with sodium citrate.⁴⁴ A comparison of the corresponding

composition–time profile with AuNP@citrate under otherwise identical conditions further emphasizes the efficacy of **3a** and **3a-PEG** as a conversion of only 22% was obtained after 40 min (Table 1 entry 14); the lower selectivity of 87% was due to formation of azoxybenzene (2%) and aniline (1%). The low activity of AuNP@citrate is entirely consistent with recent work from the Astruc group as citrate-stabilized AuNPs were shown to be much less active than those stabilized by mono, bifunctional, polymeric and dendritic 1,2,3-triazoles terminated with PEG;^{26d,f} the efficacy of these triazole-stabilized systems was attributed to weak coordination of the heteroatom donor to the nanoparticle surface and facile substitution by substrate. Furthermore, AuNPs generated by reduction of potassium tetrachloroaurate in water in the absence of stabilizer was slightly more active than its citrate-stabilized counterpart and gave 29% conversion with 89% selectivity for *N*-phenylhydroxylamine. The same nanoparticle system was also generated *in situ* and treated with polymer **1a-PEG** prior to addition of substrate to explore the influence of the stabilizer on catalyst performance. The conversion of 20% and selectivity of 84% obtained under the same conditions is slightly poorer than that obtained with AuNP@citrate, which is a strong indication that the high selectivity obtained with **3a-PEG** may result from the influence of the PIIL on NP growth. Not surprisingly a background reaction conducted by replacing catalyst **3a** with polymer **1a** gave no conversion, confirming that AuNPs were essential for catalysis.

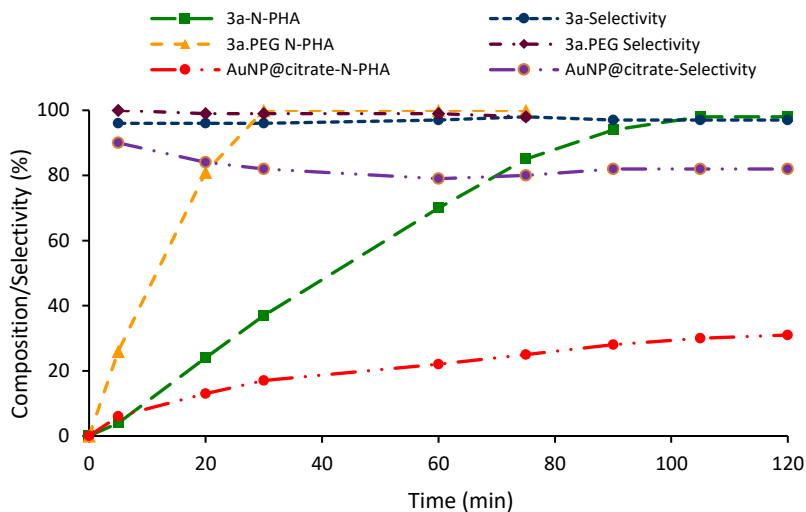


Figure 5 Reaction profile as a function of time for the selective partial reduction of nitrobenzene to *N*-phenylhydroxylamine (N-PHA) in water under nitrogen at 25 °C using 2.5 equivalents of NaBH₄ catalyzed by 0.005 mol% **3a**, **3a.PEG** or AuNP@citrate.

Finally, TEM analysis of the aqueous phase remaining after sodium borohydride-mediated reduction of nitrobenzene catalyzed by 0.005 mol% **3a.PEG** revealed that while the gold nanoparticles remained near monodisperse there was a slight increase in size with a mean diameter of 3.3 ± 1.1 nm compared to a sample examined before catalysis which had a mean diameter of 2.5 ± 0.6 nm; the micrograph and associated distribution histograms based on >100 particles is shown in the ESI (Figure S43).

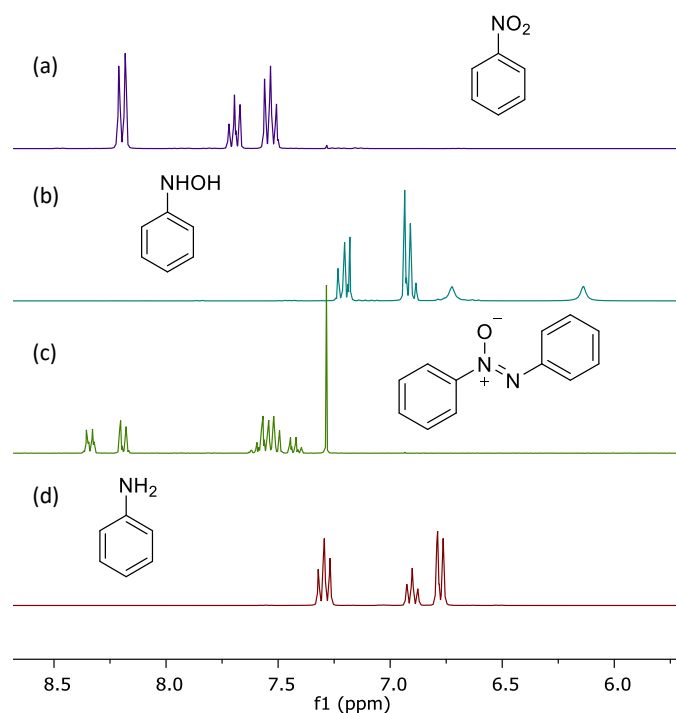


Figure 6 ^1H NMR spectra for the selective reduction of nitrobenzene catalyzed by **3a.PEG** (a) nitrobenzene, (b) *N*-phenylhydroxylamine (0.005 mol% **3a.PEG**, under nitrogen, 25 °C, 30 min, 2.5 equiv. NaBH_4 , water), (c) azoxybenzene (0.005 mol% **3a.PEG**, under nitrogen, 25 °C, 2.5 h, 2.5 equiv. NaBH_4 , ethanol) and (d) aniline (0.005 mol% **3a.PEG**, under nitrogen, 50 °C, 6 h, 5.0 equiv. NaBH_4 , water).

The influence of the diphenylphosphine and PEG components on catalyst performance has also been explored by comparing the performance of **3a** and **3a.PEG** against AuNP@PIILP (**3b**) and AuNP@PEG-PIILP (**3b.PEG**) which correspond to selective removal of the diphenylphosphino group from both. Under the same conditions a 0.005 mol% loading of **3b** gave 27% conversion and 97% selectivity for *N*-phenylhydroxylamine while the same loading of **3b.PEG** gave 55% conversion and 96% selectivity; thus, selective removal of the diphenylphosphino group results in

a significant drop in activity (Table 1 entries 15-16). In addition, the selective removal of the PEG results in a marked drop in activity as evidence by the conversions of 43% and 99% obtained with **3a** and **3a.PEG**, respectively, and 27% and 55% with **3b** and **3b.PEG**, respectively. While this may reflect an improvement in dispersibility for the PEG-based systems in water as the mean diameters of the nanoparticles in **3b** and **3b.PEG** are essentially the same (3.4 ± 1.1 and 3.3 ± 0.9 nm, respectively) it is interesting to note that the nanoparticles in the most efficient catalyst (**3a.PEG**) are significantly smaller (2.5 ± 0.6 nm) than each of the other systems examined and as such further catalyst modifications and associated studies will be required to deconvolute what factors control or influence catalyst performance.

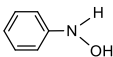
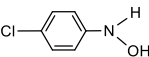
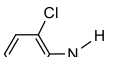
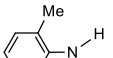
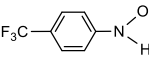
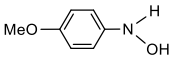
The efficacy of **3a.PEG** was further tested by reducing the catalyst loading to 0.0002 mol% and under otherwise identical conditions the conversion of 22% to *N*-phenylhydroxylamine with 100% selectivity after only 1.5 h corresponds to a turnover number (TON, measured as total moles of product per mole of catalyst) of 110,000 and a TOF of $73,000 \text{ h}^{-1}$. As this reaction is likely to be mass transfer limited due to poor solubility of the substrate, these turnover numbers are probably more representative of the potential intrinsic turnover rate of the catalyst, particularly as a further decrease in catalyst loading to 0.0001 mol% resulted in a marginal increase in TON to 112,000, in the same time. While there is a plethora of AuNP-based systems that catalyze the sodium borohydride-mediated reduction of nitroarenes,²⁶ the vast majority give complete reduction to the aniline and there are no reports of selective reduction to the corresponding *N*-arylhydroxylamine. Moreover, even though there are a few reports of catalysts that are selective for transfer hydrogenation of nitroarenes to *N*-arylhydroxylamines,³¹ these systems suffer severe limitations such as the need for a high catalyst loading, high reaction temperatures and/or long reaction times, the use of organic solvents and/or low selectivities. The high selectivity and TOF obtained with

3a.PEG in water under mild conditions at low catalyst loadings is unprecedented for a gold catalyst and the highest to be reported for the transfer hydrogenation of this class of substrate, which is quite remarkable given the challenging nature of the transformation; future studies will be directed towards understanding the origin of this efficacy. Moreover, the efficacy of **3a.PEG** even matches that of recently reported platinum-based systems that are highly selective for the hydrogenation of nitroarenes to *N*-arylhydroxylamines; both systems required surface modification with an amine-based donor to achieve high selectivity.^{11a,b} In one case, the effect was attributed to an interfacial electronic effect which favors adsorption of the reactant over the electron rich *N*-phenylhydroxylamine while the other associated the selectivity to competitive adsorption; in this regard, future studies will further explore the influence of the phosphine donor on catalyst efficacy.

The protocol developed above has been applied to the aqueous phase reduction of selected nitroarenes to assess the potential scope and efficacy of **3a.PEG**. All reactions were conducted in water and the times varied to obtain the best compromise between yield and selectivity; full details are presented in Table 2. Good conversions were obtained for 2-chloro- and 4-chloronitrobenzene which gave the corresponding *N*-(2-chlorophenyl)- and *N*-(4-chlorophenyl)hydroxylamine in 95% and 93% selectivity, respectively. Interestingly, in contrast to many palladium-based systems, there was no evidence for competing hydrodehalogenation to afford either nitrobenzene or aniline.⁴⁵ An excellent conversion and high selectivity was also obtained with 4-trifluoromethylnitrobenzene which gave *N*-(4-(trifluoromethyl)phenyl)hydroxylamine as the major product in 97% selectivity at 99% conversion, together with less than 3% of the corresponding aniline as the only other identifiably product. Similarly, under the same conditions *N*-(*o*-tolyl)hydroxylamine was reduced to the corresponding hydroxylamine *N*-(*o*-tolyl)hydroxylamine in 97% selectivity at 99% conversion. However, when the same protocol was

applied to the reduction of 1-methoxy-4-nitrobenzene, as a representative example of a nitrobenzene substituted with an electron donating group, the reaction reached 79% conversion after 2h and 68% selectivity for the desired *N*-(4-methoxyphenyl)hydroxylamine with 4-methoxyaniline as the only other significant by-product.

Table 2 Partial reduction of nitroarenes to *N*-arylhydroxylamines with NaBH₄ catalyzed by AuNP@PPh₂-PEGPIILP (**3a.PEG**).^a

Product			
Conversion ^b	>99% (1) ^c	80% (3) ^c	98% (1) ^c
Selectivity ^b	100%	93%	95%
Product			
Conversion ^b	99% (1) ^c	99% (1) ^c	79% (3) ^c
Selectivity ^b	97%	97%	68%

^a Reaction conditions: 1 mmol substrate, 0.005 mol% **3a.PEG**, under nitrogen, 2.0 mL water, 2.5 mmol NaBH₄, 25 °C, 2h. ^b Yields and selectivities determined either by ¹H NMR spectroscopy using dioxane as internal standard. Average of three runs ^c Average deviations (d) = $(|x_1 - \bar{x}| + |x_2 - \bar{x}| + |x_3 - \bar{x}|)/3$ where $\bar{x} = (x_1 + x_2 + x_3)/3$ and x_n is the conversion for run n . ^d *N*-arylhydroxylamine selectivity = $[\% \text{ } N\text{-arylhydroxylamine} / (\% \text{ } N\text{-arylhydroxylamine} + \% \text{ aniline} + \% \text{ azoxyarene})] \times 100\%$.

Selective Reduction of Nitrobenzene to Azoxybenzene and Aniline

The dramatic solvent dependent selectivity for the reduction of nitrobenzene in water and ethanol identified in our preliminary optimization above prompted us to undertake a solvent screen by varying the ethanol-water ratio to identify the composition range that affords azoxybenzene in

high selectivity. As the reduction of nitrobenzene in ethanol only reached 19% conversion after 40 min using 0.005 mol% **3a**, albeit with 100% selectivity for azoxybenzene, we chose to use **3a.PEG** for the solvent screen as it was markedly more active for the selective reduction of nitrobenzene to *N*-phenylhydroxylamine. Interesting, high selectivity for *N*-phenylhydroxylamine was retained in water/ethanol mixtures even up to an ethanol content of 99% and the switch in selectivity only occurred in dry ethanol, with 0.005 mol% **3a.PEG** giving complete conversion to afford azoxybenzene as the sole product after 2.5 h at 25 °C. Moreover, aqueous workup of this reaction mixture resulted in the appearance of a significant amount of *N*-phenylhydroxylamine, suggesting that formation of azoxybenzene is reversible in the presence of reducing agent; this was confirmed by stirring an ethanol/water solution of commercially available azoxybenzene in the presence of 0.005 mol% **3a.PEG** and 2.5 equivalents of sodium borohydride in air for 15 min and comparing the ¹H NMR spectrum of the resulting mixture with those of authentic samples. Interestingly, *N*-phenylhydroxylamine was the only product detected under these conditions which may well be due to rapid reduction of the nitrosobenzene by-product that would be generated in the hydrolysis of azoxybenzene. The efficacy of **3a-PEG** as a catalyst for the selective reduction of nitrobenzene to azoxybenzene is evident from the ¹H NMR spectrum of the reaction mixture after 2.5 h which showed complete consumption of substrate with azoxybenzene as the only spectroscopically observable product (Figure 6c).

Reduction of the catalyst loading to 0.0002 mol% gave 11% conversion to azoxybenzene as the sole product after 1.5 h at 25 °C; this corresponds to a TON of 55,000 and a TOF of 37,000 h⁻¹ which is probably more representative of the potential intrinsic turnover rate of the catalyst. The composition/selectivity-time profile for the NaBH₄-mediated selective partial reduction of

nitrobenzene to azoxybenzene in ethanol catalyzed by 0.005 mol% **3a-PEG** (Figure 7) shows that azoxybenzene is the only observable product and that 100% selectivity is retained even at complete conversion (150 min). However, when the reaction time was extended to 6 h, selectivity to azoxybenzene dropped due to the formation of azobenzene, diphenylhydrazine and aniline; which suggests that reduction may be occurring via the condensation pathway. While this product distribution is consistent with condensation, a recent experimental and computational investigation on the ruthenium nanoparticle catalyzed reduction of nitrobenzene has succinctly demonstrated that even when azoxybenzene forms, aniline is still likely to be generated via the direct pathway as formation of Ph-NH-NOH-Ph and Ph-NH-NH-Ph are both thermodynamically difficult uphill processes.¹³ In comparison to **3a-PEG**, **3a** also catalyzed the reduction of nitroarenes in ethanol with high selectivity for azoxybenzene, but only reached 29% conversion in the same time; this again may well reflect the accessibility of the active site arising from the disparate hydrophilicity and dispersibility of these catalysts. The influence of the phosphorus heteroatom donor on catalyst selectivity was also examined by comparing the performance of AuNP@PEG-PIILP and AuNP@PIILP under the same conditions. Selective removal of the PPh₂ resulted in a marked drop in activity as well as a reduction in selectivity with AuNP@PEG-PIILP giving 26% conversion and 88% selectivity while AuNP@PIILP reached 23% conversion and 65% selectivity for azoxybenzene. Finally, the efficacy of **3a-PEG** was further compared against AuNP@citrate which catalyzed the reduction under the same conditions but only reached 13% conversion after 3 days albeit with 100% selectivity for azoxybenzene. Similarly, AuNPs generated *in situ* in the absence of stabilizer were inactive under the optimum conditions.

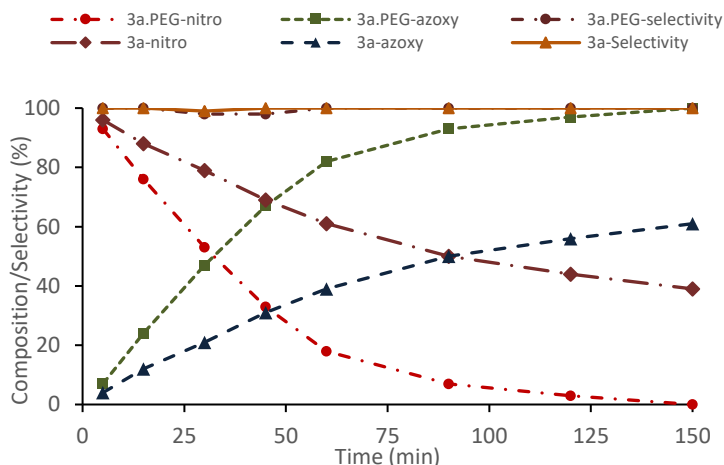


Figure 7 Reaction profile and azoxybenzene selectivity as a function of time for the partial reduction of nitrobenzene to azoxybenzene in ethanol under nitrogen at 25 °C using 2.5 equivalents of NaBH₄ and catalyzed by 0.005 mol% **3a** and **3a.PEG**.

As the reductions in water and ethanol were conducted under otherwise identical conditions, we tentatively suggest that the switch in selectivity may be associated with the markedly higher solubility of nitrobenzene in ethanol compared with water as this would result in a higher concentration of reactant on the surface of the nanoparticle which would favor condensation of two reactive species.

Complete selectivity for azoxybenzene with such a TOF under mild conditions is quite remarkable and unprecedented for a gold nanoparticle catalyst. Indeed, a survey of the literature revealed that there are a limited number of catalysts capable of reducing nitrobenzene to azoxybenzene and in each case both **3a** and **3a-PEG** outperformed these by quite some margin. For example, gold nanoparticles supported on mesostructured ceria (Au/*meso*-CeO₂) is a selectivity switchable catalyst that reduces nitroarenes with 2-propanol to the azoxyarene,

azoarene and the corresponding aniline depending on the reaction conditions.^{27b} However, a much higher catalyst loading (1 mol%) and longer reaction times were required and the TOF of 20 h⁻¹ was significantly lower than that of 37,000 h⁻¹ reported above for **3a.PEG**. Most interestingly, the high selectivity for azoxyarene was obtained in 2-propanol and addition of water resulted in a switch in selectivity to afford azoxyarene; this is in stark contrast to **3a** and **3a.PEG** which generated *N*-phenylhydroxylamine as the sole product in a 1:1 mixture of 2-propanol and water. Other systems that catalyze the selective reduction of nitrobenzene include urchin-like Ni/graphene nanocomposites that reached 100% selectivity but with a TOF of only 16.8 h⁻¹,^{37b} Ag-Cu alloy nanoparticles that catalyze selective reduction of nitroarenes to azoxy compounds through visible light irradiation with good selectivity (76-86%) but low TOFs (1-2 h⁻¹)^{37c} and iridium/rhodium-based hierarchically-coiled ultrathin nanosheets that gave azoxybenzene up to 89% selectivity and a TOF of 400 h⁻¹.^{37d}

As the majority of AuNP-based systems catalyze the reduction of nitroarenes to afford the corresponding aniline, studies were undertaken with catalyst **3a** and **3a.PEG** to establish the conditions necessary to achieve complete reduction to aniline with the aim of comparing and evaluating their efficacy against existing systems. Using the studies described above as a lead, the reduction of nitrobenzene was monitored as a function of time at 60 °C in water using 0.005 mol% **3a.PEG** and the composition quantified by ¹H NMR spectroscopy and GC. The resulting composition-time profile shown in Figure 8a shows rapid consumption of nitrobenzene with concomitant formation of *N*-phenylhydroxylamine, which is the major species after 10 min (82%), together with a minor amount of aniline (14%). Longer reaction times resulted in consumption of *N*-phenylhydroxylamine to afford aniline which was ultimately obtained in quantitative yield after 180 min. Not surprisingly, the corresponding composition-time profile obtained with catalyst **3a**

is qualitatively similar (Figure 8b) although complete conversion to aniline required significantly longer. Both composition-time profiles are indicative of reaction via the direct pathway as there is no evidence for the formation of azoxy intermediates. In stark contrast, azoxybenzene, diphenylhydrazine and *N*-phenylhydroxylamine have all been identified during the reduction of nitrobenzene with gold nanoparticles supported on imidazolium-based porous organic polymers; however, these studies appear to have been conducted in air which may be the origin of the vastly disparate composition profiles.^{26h} Finally, when the catalyst loading was reduced to 0.0002 mol% complete reduction to aniline could be obtained after only 8 h at 50 °C, this corresponds to a TON of 500,000 and a TOF of 62,500 h⁻¹ (based on total gold content). Although the poor solubility of the substrate undoubtedly limits this TOF, comparison with related NP-based systems that also operate under mass transfer control reveals it to be among the most active gold nanoparticle-based systems to be reported for the aqueous phase transfer hydrogenation of nitroarenes. The efficacy of **3a.PEG** may well be associated with the electrostatic potential around the AuNPs as favorable electrostatic interactions between positively charged ([+])-AuNPs and negatively charged substrates has been demonstrated to be responsible for enhancing the rate of reduction of nitroarenes by channeling the substrate to the NP surface.^{46a} In this system, AuNPs modified with positively charged thiolates, ([+])-AuNP, gave complete reduction of 4-nitrophenolate and 4-nitroaniline at room temperature in only 10 min with a catalyst loading of 0.1 mol% whereas its negatively charged counterpart ([-]) AuNPs failed to catalyze the same reductions even after 2 days. In a related concept, the approach of charged substrates such as nitroarenes to the surface of a nanoparticle catalyst has recently been reported to be controlled by the size of the counterions surrounding charged on-particle ligands.^{46b}

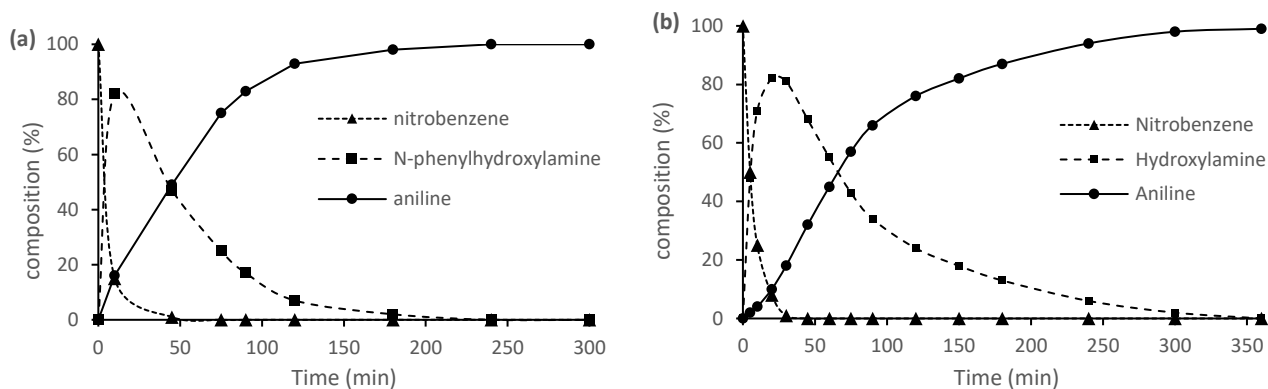
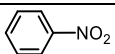
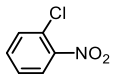
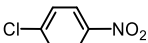
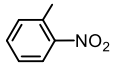
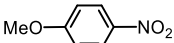
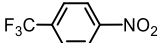
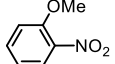
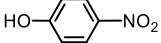
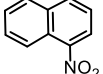


Figure 8 Reaction profiles as a function of time for the reduction of nitrobenzene in water under nitrogen at 60 °C using 5.0 mole equivalents of NaBH₄ showing direct reduction to aniline via *N*-phenylhydroxylamine to be the major pathway (a) 0.005 mol% **3a.PEG** and (b) 0.005 mol% **3a**.

The protocol developed above for reduction of nitrobenzene to aniline has also been extended to a selection of electron rich and electron poor substrates which all gave high conversion to afford the corresponding aniline as the sole product after relatively short reaction times (4-6 h) (Table 3). Gratifyingly, reduction of 1-chloro-4-nitrobenzene and 1-chloro-2-nitrobenzene occurred with high selectivity to afford 4-chloro and 2-chloroaniline, respectively, with no evidence for hydrodechlorination to afford aniline. Nitroarenes substituted at the 2-position were also converted to the corresponding aniline in high yield and 100% selectivity, albeit after slightly longer reaction times due to steric hindrance inhibiting access of the substrate to the catalyst surface. Similarly, while reduction of 1-nitronaphthalene was sluggish under the same conditions, complete conversion to 1-aminonaphthalene could be obtained after only 6 h when the reaction temperature was raised to 70 °C.

Table 3 Sodium borohydride mediated reduction of nitroarenes to the corresponding aniline catalyzed by AuNP@PPh₂-PEGPIILP (**3a.PEG**).^a

substrate	Time	Conv. (%) / Select. (%) ^b
	2h	99/100
	5h	100/100
	5h	100/100
	5h	99/100
	4h	98/100
	5h	98/100
	6h	97/99
	4h	100/100
	6h	>99/100

^a Reaction conditions: 1 mmol substrate, 0.005 mol% **3a.PEG**, 2.0 mL water, under nitrogen, 5.0 mmol NaBH₄, 50 °C, reaction time given in parentheses after conversions (h). ^b Yields determined by ¹H NMR spectroscopy using dioxane as internal standard. Average of three runs.

CONCLUSIONS

Gold nanoparticle catalysts stabilized by phosphine-decorated polymer immobilized ionic liquids are exceptionally efficient catalysts for the partial and complete reduction of nitrobenzene and give unprecedentedly high activities and selectivities for *N*-phenylhydroxylamine,

azoxybenzene and aniline. Reductions conducted in water under mild conditions at low catalyst loadings afford *N*-phenylhydroxylamine in quantitative yields and >99% selectivity while the use of ethanol as solvent, under otherwise identical conditions, results in a dramatic switch in selectivity to afford azoxybenzene as the sole product. The composition-selectivity profiles for the partial reduction of nitrobenzene raises a number of searching and pertinent questions about the origin of the selectivity and the mechanism of reduction and further *in situ* surface spectroscopic investigations as well as kinetic and computational studies will be required to develop a full understanding of this system. As both the phosphine and ionic liquid components are required for optimum efficacy future studies on modified catalyst systems will be undertaken to explore whether the electronic structure of the gold nanoparticles and/or the electrostatic potential around the AuNPs are selectivity and activity determining. The modular construction of the PIIL supports will lend itself to modifying properties such as ionic microenvironment and surface potential, the density of heteroatom donors, hydrophilicity, porosity and mechanical integrity and thereby substrate accessibility, catalyst surface interactions and ultimately catalyst efficacy. In particular, PIILP-based systems are ideally suited to explore the role of electrostatic interactions in the reduction of charged substrates with the aim of developing smart catalysts with enzymatic activity and selectivity. We are currently using our optimum catalyst to develop a continuous flow process for the scale-up synthesis of *N*-phenylhydroxylamine and azoxybenzene as both intermediates to industrially important value-added products.

ASSOCIATED CONTENT

Supporting Information

The Supporting Information is available free of charge on the ACS Publications website at DOI: 10.1021/acscatal.XXXXXXXXXX

Synthesis and characterization of AuCl₄-loaded co-polymers **2a**, **2a.PEG**, **3b** and **2b.PEG**, TGA and DSC curves for **1a**, **1a.PEG**, **1b** and **1b.PEG** (PDF), SEM images for **2a**, **2a.PEG**, **2b** and **2b.PEG** (PDF), TEM images of **3a**, **3a.PEG**, **3b** and **3b.PEG** (PDF), FTIR traces (PDF) and X-ray photoelectron spectra for **2a**, **2a.PEG**, **2b**, **2b.PEG**, **3a**, **3a.PEG**, **3b** and **3b.PEG** (PDF).

AUTHOR INFORMATION

Corresponding Author

*E-mail: simon.doherty@ncl.ac.uk

*E-mail: j.g.knight@ncl.ac.uk

*E-mail: T.W.Chamberlain@Leeds.ac.uk

ORCID

Simon Doherty: 0000-0003-1103-8090

Julian Knight: 0000-0002-1120-8259

Richard Bourne: 0000-0001-7107-6297

Thomas Chamberlain: 0000-0001-8100-6452

Christopher Hardacre: 0000-0001-7256-6765

Notes

The authors declare no competing financial interest.

ACKNOWLEDGMENT

We gratefully acknowledge Newcastle University for financial support (TB). Solid state ^{31}P and ^{13}C NMR spectra were recorded and interpreted by Dr Nick Reese at Oxford University, XPS data was obtained at the EPSRC National Facility for X-Ray Photoelectron Spectroscopy located in the Research Complex at Harwell. We also thank Dr Kathryn White for the SEM images (Faculty of Medical Sciences, Newcastle University).

REFERENCES

(1) (a) Sheldon, R. A.; Van Bekkum, H. *Fine Chemicals through Heterogeneous Catalysis*, Wiley, Weinheim, 2008. (b) Noyori, R. Synthesizing our Future. *Nature Chem.* **2009**, *1*, 5–6. (c) Samorjai, G. A.; Rioux, R. M. High Technology Catalysts Towards 100% selectivity: Fabrication, Characterization and Reaction Studies. *Catal. Today* **2005**, *100*, 201–215.

(2) (a) Van Leeuwen, P. N. M. W. *Homogeneous Catalysis: Understanding the Art*. Kluwer, Dordrecht, 2004. (b) Wang, D.-H.; Engle, K. M.; Shi, B.-F.; Yu, J.-Q. Ligand-Enabled Reactivity and Selectivity in a Synthetically Versatile Aryl C-H Olefination. *Science* **2010**, *327*, 315–319. (c) Börner, A. *Phosphorus Ligands in Asymmetric Catalysis: Synthesis and Applications*, Wiley-VCH, Weinheim, 2008. (d) Gillespie, J. A.; Zuidema, E.; van Leeuwen, P. W. N. M.; Kamer, P. J. C. *Phosphorus Ligand Effects in Homogenous Catalysis and Rational Catalyst Design*, Wiley, Chichester, 2012. (e) Kerr, W. J.; Mudd, R. J.; Brown, J. A. Iridium(I) N-Heterocyclic Carbene (NHC)/Phosphine Catalysts for Mild and Chemoselective Hydrogenation Processes. *Chem. Eur. J.* **2016**, *22*, 4738–4742.

(3) (a) Astruc, D.; Lu, F.; Aranzaes, J. R. Nanoparticles as Recyclable Catalysts: The Frontier Between Homogeneous and Heterogeneous Catalysis. *Angew. Chem. Int. Ed.* **2005**, *44*, 7852–

7872. For examples of ligand controlled selectivity in heterogeneous catalysis see: (b) Kunz, S.; Schreiber, P.; Ludwig, M.; Maturi, M. M.; Ackermann, O.; Tschurl, M.; Heiz, U. Rational Design, Characterization and Catalytic Application of Metal Clusters Functionalized with Hydrophilic, Chiral Ligands: A Proof of Principle Study. *Phys. Chem. Chem. Phys.* **2013**, *15*, 19253–19261. (c) Witte, P. T.; Berben, P. H.; Boland, S.; Boymans, E. H.; Vogt, D.; Geus, J. W.; Donkervoot, J. G. BASF NanoSelect™ Technology: Innovative Supported Pd- and Pt-Based Catalysts for Selective Hydrogenation Reactions. *Top. Catal.* **2012**, *55*, 505–511.

(4) (a) Medlin, J. W. Controlling the Surface Environment of Heterogeneous Catalysts Using Self-Assembled Monolayers. *Acc. Chem. Res.* **2013**, *47*, 1438–1445. (b) Marshall, S. T.; O'Brien, M.; Oetter, B.; Corpuz, B.; Richards, R. M.; Schwartz, D. K.; Medlin, J. W. Controlled Selectivity for Palladium Catalysts Using Self-assembled Monolayers. *Nature Materials* **2010**, *9*, 853–858. (c) Kahsar, K. R.; Schwartz, D. K.; Medlin, J. W. Control of Metal Catalyst Selectivity Through Specific Noncovalent Molecular Interactions. *J. Am. Chem. Soc.* **2014**, *136*, 520–526. (d) Albani, D.; Vile, G.; Mitchell, S.; Witte, P. T.; Almora-Barrios, N.; Verel, R.; Lopez, N.; Perez-Ramirez, J. Ligand Ordering Determines the Catalytic Response of Hybrid Palladium Nanoparticles in Hydrogenation. *Catal. Sci. Technol.* **2016**, *6*, 1621–1631. (e) Wu, B.; Huang, H.; Yang, J.; Zheng, N.; Fu, G. Selective Hydrogenation of α,β -Unsaturated Aldehydes Catalyzed by Amine-Capped Platinum-Cobalt Nanocrystals. *Angew. Chem. Int. Ed.* **2012**, *51*, 3440–3443. (f) Chen, K.; Wu, H.; Hua, Q.; Chang, S.; Huang, W. Enhancing Catalytic Activity of Supported Metal Nanoparticles with Capping Ligands *Phys. Chem. Chem. Phys.* **2013**, *15*, 2273–2277.

(5) Snelders, D. J. M.; Yan, N.; Gan, W.; Laurency, G.; Dyson, P. J. Tuning the Chemoselectivity of Rh Nanoparticle Catalysts by Site-Selective Poisoning with Phosphine

Ligands: The Hydrogenation of Functionalized Aromatic Compounds. *ACS Catal.* **2012**, *2*, 201–207.

(6) Fedorov, A.; Liu, H.-J.; Lo, H.-K.; Copèret, C. Tunable Heterogeneous Catalysis: N-Heterocyclic Carbenes as Ligands for Supported Heterogeneous Ru/K-Al₂O₃ Catalysts to Tune Reactivity and Selectivity. *J. Am. Chem. Soc.* **2016**, *138*, 16502–16507.

(7) (a) Cano, I.; Chapman, A. M.; Urakawa, A.; van Leeuwen, P. W. M. N. Air-Stable Gold Nanoparticles Ligated by Secondary Phosphine Oxides for the Chemoselective Hydrogenation of Aldehydes: Crucial Role of the Ligand. *J. Am. Chem. Soc.* **2014**, *136*, 2520–2528. (b) Almora-Barrios, N.; Cano, I.; van Leeuwen, P. W. M. N.; Lopez, N. Concerted Chemoselective Hydrogenation of Acrolein on Secondary Phosphine Oxide Decorated Gold Nanoparticles. *ACS Catal.* **2017**, *7*, 3949–3954. (c) Cano, I.; Huertos, M. A.; Chapman, A. M.; Buntkowsky, G.; Gutmann, T.; Groszewicz, P. B.; van Leeuwen, P. W. M. N. Air-Stable Gold Nanoparticles Ligated by Secondary Phosphine Oxides as Catalyst for the Chemoselective Hydrogenation of Substituted Aldehydes: a Remarkable Ligand Effect. *J. Am. Chem. Soc.* **2015**, *137*, 7718–7727.

(8) Castlebou, J. L.; Bresó-Femenia, E.; Blondeau, P.; Chaudret, B.; Castellón, S.; Claver, C.; Cyril, G. Tuning the Selectivity in the Hydrogenation of Aromatic Ketones Catalyzed by Similar Ruthenium and Rhodium Nanoparticles. *ChemCatChem* **2014**, *6*, 3160–3168.

(9) Castlebou, J. L.; Gual, A.; Mercadè, E.; Claver, C.; Godard, C. Ligand Effect in the Rh-NP Catalysed Partial Hydrogenation of Substituted Arenes. *Catal. Sci. Technol.* **2013**, *3*, 2828–2833.

(10) Jayakumar, S.; Modak, A.; Guo, M.; Li, H.; Hu, X.; Yang, Q. Ultrasmall Platinum Stabilized on Triphenylphosphine-Modified Silica for Chemoselective Hydrogenation. *Chem. Eur. J.* **2017**, *23*, 7791–7797.

(11) (a) Chen, G.; Xu, C.; Huang, X.; Ye, J.; Gu, L.; Li, G.; Tang, Z.; Wu, B.; Yang, H.; Zho, Z.; Zhou, Z.; Fu, G.; Zheng, N. Interfacial Electronic Effects Control the Reaction Selectivity of Platinum Catalysts. *Nature Materials* **2016**, *15*, 564–569. (b) Boymans, E. H.; Witte, P. T.; Vogt, D. A Study on the Selective Hydrogenation of Nitroaromatics to N-Arylhydroxylamines using a Supported Pt Nanoparticle Catalyst. *Catal. Sci. Technol.* **2015**, *5*, 176–183.

(12) (a) Tan, J.; Cui, J.; Ding, G.; Deng, T.; Zhu, Y.; Li, Y.-W. Efficient Aqueous Hydrogenation of Levulinic Acid to γ -Valerolactone over a Highly Active and Stable Ruthenium Catalyst. *Catal. Sci. Technol.* **2016**, *6*, 1469–1475. (b) Michel, C.; Gallezot, P. Why Is Ruthenium an Efficient Catalyst for the Aqueous-Phase Hydrogenation of Biosourced Carbonyl Compounds? *ACS Catal.* **2015**, *5*, 4130–4132.

(13) Mondal, J.; Kundu, S. K.; Kwok, Hung Ng, W. K.; Singuru, R.; Borah, P.; Hirao, H.; Zhao, Y.; Bhaumik, A. Fabrication of Ruthenium Nanoparticles in Porous Organic Polymers: Towards Advanced Heterogeneous Catalytic Nanoreactors. *Chem. Eur. J.* **2015**, *21*, 19016–19027.

(14) Guo, M.; Li, C.; Yang, Q. Accelerated Catalytic Activity of Pd NPs Supported on Amine-Rich Silica Hollow Nanospheres for Quinoline Hydrogenation. *Catal. Sci. Technol.* **2017**, *7*, 2221–2227.

(15) (a) Kwon, S. G.; Krylova, G.; Sumer, A.; Schwartz, M. M.; Bunel, E. E.; Marshall, C. L.; Chattopadhyay, S.; Lee, B.; Jellinek, J.; Shevchenko, E. V. Capping Ligands as Selectivity Switchers in Hydrogenation Reactions, *Nano. Lett.* **2012**, *12*, 5382–5388. (b) Long, W.; Brunelli, N. A.; Didas, S. A.; Ping, E. W.; Jones, C. W. Aminopolymer–Silica Composite-Supported Pd Catalysts for Selective Hydrogenation of Alkynes. *ACS. Catal.* **2013**, *3*, 1700–1708. (c) da. Silva, F. P.; Fiorio, J. L.; Rossi, L. M. Tuning the Catalytic Activity and Selectivity of Pd Nanoparticles

Using Ligand-Modified Supports and Surfaces. *ACS Omega* **2017**, *2*, 6014–6022. (d) Guo, Z.; Xiao, C.; Maligal-Ganesh, R. V.; Zhou, L.; Goh, T. W.; Li, X.; Tesfagaber, D.; Thiel, A.; Huang, W. Pt Nanoclusters Confined within Metal–Organic Framework Cavities for Chemoselective Cinnamaldehyde Hydrogenation. *ACS Catal.* **2014**, *4*, 1340–1348.

(16) Schrader, I.; Warneke, J.; Backenkohler, J.; Kunz, S. Functionalization of Platinum Nanoparticles with L-Proline: Simultaneous Enhancements of Catalytic Activity and Selectivity. *J. Am. Chem. Soc.* **2015**, *137*, 905–912.

(17) Liu, H.; Mei, Q.; Li, S.; Yang, Y.; Wang, Y.; Liu, H.; Zheng, L.; An, P.; Zhang, J.; Han, B. Selective Hydrogenation of Unsaturated Aldehydes over Pt Nanoparticles Promoted by the Cooperation of Steric and Electronic Effects. *Chem. Commun.* **2018**, *54*, 908–911.

(18) Ernst, J. B.; Schwermann, C.; Yokota, G.; Tada, M.; Muratsugu, S.; Doltsinis, N. L.; Glorius, F. Molecular Adsorbates Switch on Heterogeneous Catalysis: Induction of Reactivity by N-Heterocyclic Carbenes. *J. Am. Chem. Soc.* **2017**, *139*, 9144–9147.

(19) Ernst, J.; Muratsugu, S.; Wang, F.; Tada, M.; Glorius, F. Tunable Heterogeneous Catalysis: N-Heterocyclic Carbenes as Ligands for Supported Heterogeneous Ru/K-Al₂O₃ Catalysts to Tune Reactivity and Selectivity. *J. Am. Chem. Soc.* **2016**, *138*, 10718–10721.

(20) (a) Martínez-Prieto, L. M.; Ferry, A.; Rakers, L.; Richter, C.; Lecante, P.; Philippot, K.; Chaudret, B.; Glorius, F. Long-chain NHC-stabilized RuNPs as Versatile Catalysts for One-pot Oxidation/Hydrogenation Reactions. *Chem. Commun.* **2016**, *52*, 4768–4771. (b) Richter, C.; Schaepe, K.; Glorius, F.; Ravoo, B. J. Tailor-Made N-Heterocyclic Carbenes for Nanoparticle Stabilization. *Chem. Commun.* **2014**, *50*, 3204–3207. (c) Lara, P.; Martínez-Prieto, L. M.; Roselló-Merino, M.; Richter, C.; Glorius, F.; Conejero, S.; Philippot, K.; Chaudret, B. NHC-Stabilized Ru

Nanoparticles: Synthesis and Surface Studies. *Nano-Struct. Nano-Obj.* **2016**, *6*, 39–45. (d) Rühling, A.; Schaepe, K.; Rakers, L.; Vonhören, B.; Tegeder, P.; Ravoo, B. J.; Glorius, F. Modular Bidentate Hybrid NHC-Thioether Ligands for the Stabilization of Palladium Nanoparticles in Various Solvents. *Angew. Chem. Int. Ed.* **2016**, *55*, 5856–5860. (e) Ferry, A.; Schaepe, K.; Tegeder, P.; Richter, C.; Chepiga, K. M.; Ravoo, B. J.; Glorius, F. Negatively Charged N-Heterocyclic Carbene-Stabilized Pd and Au Nanoparticles and Efficient Catalysis in Water. *ACS Catal.* **2015**, *5*, 5414–5420.

(21) For a relevant and insightful review article see: (a) Giacalone, F.; Gruttadauria, M. Covalently Supported Ionic Liquid Phases: An Advanced Class of Recyclable Catalytic Systems. *ChemCatChem* **2016**, *8*, 664–684. See also (b) Qian, W.; Texter, J.; Yan, F. Frontiers in Poly(ionic liquids): Syntheses and Applications. *Chem. Soc. Rev.* **2017**, *46*, 1124–1159.

(22) For a relevant review see: Luska K. L; Moores, A. Functionalized Ionic Liquids for the Synthesis of Metal Nanoparticles and their Application in Catalysis. *ChemCatChem* **2012**, *4*, 1534–1546. For examples of nanoparticles stabilized by heteroatom donor modified ionic liquids see the following. Amines: (a) Zhang, A.; Cui, H. Synthesis and Characterization of Functionalized Ionic Liquid-Stabilized Metal (Gold and Platinum) Nanoparticles and Metal Nanoparticle/Carbon Nanotube Hybrids. *Langmuir* **2009**, *25*, 2604–2612. Nitriles: (b) Zhao, D. B.; Fei, Z. F.; Geldbach, T. J.; Scopelliti, R. Dyson, P. J. Nitrile-Functionalized Pyridinium Ionic Liquids: Synthesis, Characterization, and Their Application in Carbon–Carbon Coupling Reactions. *J. Am. Chem. Soc.* **2004**, *126*, 15876–15882. (c) Chiappe, C.; Pieraccini, D.; Zhao D.; Fei, Z.; Dyson, P. J. Remarkable Anion and Cation Effects on Stille Reactions in Functionalised Ionic Liquids. *Adv. Synth. Catal.* **2006**, *348*, 68–74. (d) Prechtel, M. H. G.; Scholten J. D.; Dupont, J. Tuning the Selectivity of Ruthenium Nanoscale Catalysts with Functionalised Ionic Liquids: Hydrogenation

of Nitriles. *J. Mol. Cat. A: Chem.*, **2009**, *313*, 74-78. Thiolate: (e) Itoh, H.; Maka, K.; Chujo, Y. Synthesis of Gold Nanoparticles Modified with Ionic Liquid Based on the Imidazolium Cation. *J. Am. Chem. Soc.* **2004**, *126*, 3026–3027. (f) Kocharova, N.; Leiro, J.; Lukkari, J.; Heinonen, M.; Skála, T.; Šutara, F.; Skoda, M.; Vondráček, M. Self-Assembled Carbon Nanotubes on Gold: Polarization-Modulated Infrared Reflection–Absorption Spectroscopy, High-Resolution X-ray Photoemission Spectroscopy, and Near-Edge X-ray Absorption Fine Structure Spectroscopy Study. *Langmuir* **2008**, *24*, 3235–3242. Bipyridine: (g) Léger, B.; Denicourt-Nowicki, A.; Roucoux, A.; H. Olivier-Bourbigou, H. Synthesis of Bipyridine-Stabilized Rhodium Nanoparticles in Non-Aqueous Ionic Liquids: A New Efficient Approach for Arene Hydrogenation with Nanocatalysts. *Adv. Synth. Catal.* **2008**, *350*, 153–159. (h) Léger, B.; Denicourt-Nowicki, A.; Olivier-Bourbigou, H.; Roucoux, A. Rhodium Nanocatalysts Stabilized by Various Bipyridine Ligands in Nonaqueous Ionic Liquids: Influence of the Bipyridine Coordination Modes in Arene Catalytic Hydrogenation. *Inorg. Chem.* **2008**, *47*, 9090–9096. (i) Dykeman, R. R.; Yan, N.; Scopelliti, R.; Dyson, P. J. Enhanced Rate of Arene Hydrogenation with Imidazolium Functionalized Bipyridine Stabilized Rhodium Nanoparticle Catalysts. *Inorg. Chem.* **2011**, *50*, 717–719. Hydroxyl: (j) Yan, N.; Yang, X.; Fei, Z.; Li, Y.; Kou, Y.; Dyson, P. J. Solvent-Enhanced Coupling of Sterically Hindered Reagents and Aryl Chlorides using Functionalized Ionic Liquids. *Organometallics* **2009**, *28*, 937–939. Phosphine: (k) Leal, B. C.; Consorti, C. S.; Machado, G.; Dupont, J. Palladium Metal Nanoparticles Stabilized by Ionophilic Ligands in Ionic Liquids: Synthesis and Application in Hydrogenation Reactions. *Catal. Sci. Technol.* **2015**, *5*, 903–909. (l) Luska, K. L.; Moores, A. Improved Stability and Catalytic Activity of Palladium Nanoparticle Catalysts using Phosphine-Functionalized Imidazolium Ionic Liquids *Adv. Synth. Catal.* **2011**, *353*, 3167–3177. (m) Bahadorikhalili, S.; Ma’mani, L.; Mahdavi, H.; Shafiee, A. Palladium

Catalyst Supported on PEGylated Imidazolium-Based Phosphinite Ionic Liquid-Modified Magnetic Silica Core–Shell Nanoparticles: A Worthy and Highly Water-Dispersible Catalyst for Organic Reactions in Water. *RSC Adv.* **2015**, *5*, 71297–71305.

(23) Doherty, S.; Knight, J. G.; Backhouse, T.; Abood, E.; Al-shaikh, H.; Fairlamb, I. J. S.; Bourne, R. A.; Chamberlain, T. W.; Stones, R. Highly Efficient Aqueous Phase Chemoselective Hydrogenation of α,β -Unsaturated Aldehydes Catalyzed by Phosphine-Decorated Polymer Immobilized IL-Stabilized PdNPs. *Green Chem.* **2017**, *19*, 1635–1641.

(24) Doherty, S.; Knight, J. G.; Backhouse, T.; Bradford, A.; Saunders, F.; Bourne, R. A.; Chamberlain, T. W.; Stones, R.; Clayton, A.; Lovelock, K. Highly Efficient Aqueous Phase Reduction of Nitroarenes Catalyzed by Phosphine-Decorated Polymer-Immobilized Ionic Liquid Stabilized PdNPs. *Catal. Sci. Technol.* **2018**, *8*, 1454–1467.

(25) Doherty, S.; Knight, J. G.; Backhouse, T.; Abood, E.; Al-shaikh, A.; Clemmet, A. R.; Ellison, J. R.; Bourne, R. A.; Chamberlain, T. W.; Stones, R.; Warren, N. J.; Fairlamb, I. J. S.; Lovelock, K. Heteroatom Donor-Decorated Polymer-Immobilized Ionic Liquid Stabilized Palladium Nanoparticles: Efficient Catalysts for Room-Temperature Suzuki-Miyaura Cross-Coupling in Aqueous Media. *Adv. Synth. Catal.* **2018**, *360*, 3716–3731.

(26) For relevant review articles see: (a) Zhao, P.; Feng, X.; Huang, D.; Yang, G.; Astruc, D. Basic Concepts and Recent Advances in Nitrophenol Reduction by Gold- and Other Transition Metal Nanoparticles. *Coord. Chem. Rev.* **2015**, *287*, 114–136. (b) Mitsudome, T.; Kaneda, K. Gold Nanoparticle Catalysts for Selective Hydrogenations. *Green Chem.* **2013**, *15*, 2636–2654. (c) Serna, P.; Corma, A. Transforming Nano Metal Nonselective Particulates into Chemoselective Catalysts for Hydrogenation of Substituted Nitrobenzenes. *ACS Catal.* **2015**, *5*, 7114–7121. For

selected articles see: (d) Li, N.; Echeverría, M.; Moya, S.; Ruiz, J.; Astruc, D. “Click” Synthesis of Nona-PEG-branched Triazole Dendrimers and Stabilization of Gold Nanoparticles That Efficiently Catalyze p-Nitrophenol Reduction. *Inorg. Chem.* **2014**, *53*, 6954-6961. (e) Wang, C.; Salmon, L.; Li, Q.; Igartua, M. E.; Moya, S.; Ciganda, R.; Ruiz, J.; Astruc, D. From Mono to Tris-1,2,3-triazole-Stabilized Gold Nanoparticles and Their Compared Catalytic Efficiency in 4-Nitrophenol Reduction. *Inorg. Chem.* **2016**, *55*, 6776-6780. (f) Ciganda, R.; Li, N.; Deraedt, C.; Gatard, S.; Zhao, P.; Salmon, L.; Hernández, R.; Ruiz, J.; Astruc, D. Gold Nanoparticles as Electron Reservoir Redox Catalysts for 4-Nitrophenol Reduction: a Strong Stereoelectronic Ligand Influence. *Chem. Commun.* **2014**, *50*, 10126-10129. (g) Wang, C.; Ciganda, R.; Salmon, L.; Gregurec, D.; Irigoyen, J. Highly Efficient Transition Metal Nanoparticle Catalysts in Aqueous Solutions. *Angew Chem. Int. Ed.* **2016**, *55*, 3091–3095. (h) Su, Y.; Li, X.; Wang, Y.; Zhong, H.; Wang, R. Gold Nanoparticles Supported by Imidazolium-Based Porous Organic Polymers for Nitroarene Reduction. *Dalton Trans.* **2016**, *45*, 16896-16903. (i) Gao, X.; Xu, G.; Zhao, Y.; Li, S.; Shi, F.; Chen, Y. Self-assembly of Amine-Functionalized Gold Nanoparticles on Phosphonate-Functionalized Graphene Nanosheets: A Highly Active Catalyst for the Reduction of 4-Nitrophenol. *RSC Adv.* **2015**, *5*, 88045-88051. (j) Dong, H.; Zhang, X.; Zhang, Z.; Fu, S.; Zhong, Z. The Influence of Amine Structures on the Stability and Catalytic Activity of Gold Nanoparticles Stabilized by Amine-Modified Hyperbranched Polymers. *Nanotechnology* **2018**, *29*, 055705. (k) Kureha, T.; Nagase, Y.; Suzuki, D. High Reusability of Catalytically Active Gold Nanoparticles Immobilized in Core–Shell Hydrogel Microspheres. *ACS Omega* **2018**, *3*, 6158–6165. (l) Ortega-Muñoz, M.; Blanco, V.; Henrandez-Mateo, F.; Lopez-Jaramillo, F. J.; Santoyo-Gonzalez, F. Catalytic Materials Based on Surface Coating with Poly(ethyleneimine)-Stabilized Gold Nanoparticles. *ChemCatChem* **2017**, *9*, 3965-3973.

(27) (a) Kim, J. H.; Park, J. H.; Chung, Y. K.; Park, K. H. Ruthenium Nanoparticle-Catalyzed, Controlled and Chemoselective Hydrogenation of Nitroarenes using Ethanol as a Hydrogen Source. *Adv. Synth. Catal.* **2012**, *354*, 2412–2148. (b) Liu, X.; Ye, S.; Li, H.-Q.; Liu, Y.-M.; Cao, Y.; Fan, K.-N. Mild, Selective and Switchable Transfer Reduction of Nitroarenes Catalyzed by Supported Gold Nanoparticles. *Catal. Sci. Technol.* **2013**, *3*, 3200–3206.

(28) (a) Vyas, P. M.; Roychowdhury, S.; Woster, P. M.; Svensson, C. K. Reactive oxygen species generation and its role in the differential cytotoxicity of the arylhydroxylamine metabolites of sulfamethoxazole and dapsone in normal human epidermal keratinocytes. *Biochem. Pharmacol.* **2005**, *70*, 275–286. (b) Yadav, J. S.; Reddy, B. V. S.; Streedhar, P. Three-Component One-Pot Synthesis of α -Hydroxylamino Phosphonates using Ionic Liquids. *Adv. Synth. Catal.* **2003**, *345*, 564–567. (c) Svensson, C. K. Do Arylhydroxylamine Metabolites Mediate Idiosyncratic Reactions Associated with Sulfonamides? *Chem. Res. Toxicol.* **2003**, *16*, 1034–1043. (d) Nio, D.; Zhao, K. Concerted Conjugate Addition of Nucleophiles to Alkenoates. Part I: Mechanism of N-Alkylhydroxylamine Additions. *J. Am. Chem. Soc.* **1999**, *121*, 2456–2459.

(29) Perez, V. V.; Martin, J. F.; Roling, P. V. EP0240297, 1987.

(30) (a) Ram, R. N.; Soni, V. K. Synthesis of 3-Alkylbenzoxazolones from N-Alkyl-N-arylhydroxylamines by Contiguous O-Trichloroacetylation, Trichloroacetoxy ortho-Shift, and Cyclization Sequence. *J. Org. Chem.* **2013**, *78*, 11935–11947. (b) Bamberger, E. *Ber. Dtch. Chem. Ges.* **1894**, *27*, 1548-1557. (c) Wang, Y. A.; Ye, L. W.; Zhang, L. M. Au-Catalyzed Synthesis of 2-Alkylindoles from N-Arylhydroxylamines and Terminal Alkynes. *Chem. Commun.* **2011**, *47*, 7815–7817.

(31) (a) Shi, Q. X.; Lu, R. W.; Jin, K.; Zhang, Z. X.; Zhao, D. F. Ultrasound-Promoted Highly Chemoselective Reduction of Aromatic Nitro Compounds to the Corresponding *N*-Arylhydroxylamines Using Zinc and HCOONH₄ in CH₃CN. *Chem. Lett.* **2006**, *35*, 226–227. (b) Ung, S.; Flguières, A.; Guy, A.; Ferroud, C. Ultrasonically Activated Reduction. *Tet. Lett.* **2005**, *46*, 5913–5917. (c) McGill, A. D.; Zhang, W.; Wittbordt, J.; Wang, J.; Schlegel, H. B.; Wang, P. G. *para*-Substituted *N*-Nitroso-*N*-Oxybenzenamine Ammonium Salts: A New Class of Redox-Sensitive Nitric Oxide Releasing Compounds. *Bioorg. Med. Chem.* **2000**, *8*, 405–412. (d) Barta, M.; Romea, P.; Urpi, F.; Vilarrasa, J. A Fast Procedure for the Reduction of Azides and Nitro Compounds Based on the Reducing Ability of Sn(SR)₃-Species. *Tetrahedron* **1990**, *46*, 587–594.

(32) (a) Oxley, P. W.; Adger, B. M.; Sasse, M. J.; Forth, M. A. *N*-Acetyl-*N*-Phenylhydroxylamine via Catalytic Transfer Hydrogenation of Nitrobenzene Using Hydrazine and Rhodium on Carbon. *Org. Synth.* **1989**, *67*, 187–192. (b) Entwistle, I. D.; Gilkerson, T.; Johnstone, R. A. W.; Telford, R. P. Rapid Catalytic Transfer Reduction of Aromatic Nitro Compounds to Hydroxylamines. *Tetrahedron* **1978**, *34*, 213–215. (c) Pernoud, L.; Candy, J. P.; Didillon, B. Jacquot, R.; Basset, J. M. Selective Hydrogenation of Nitrobenzene into Phenylhydroxylamine on Silica Supported Platinum Catalysts. *Studies in Surf. Sci. and Catal.* **2000**, *130*, 2057–2062. (d) Jawale, D. J.; Gravel, E.; Boudet, C.; Shah, N.; Geertsen, V.; Li, H.; Namboothiri, I. N. N. Doris, E. Selective Conversion of Nitroarenes using a Carbon Nanotube-Ruthenium Nanohybrid. *Chem. Commun.* **2015**, *51*, 1739–1742. (e) Tyler, J. H.; Nazari, S. H.; Patterson, R. H.; Udumula, V.; Smith, S. J. Synthesis of *N*-Aryl and *N*-Heteroaryl Hydroxylamines via Partial Reduction of Nitroarenes with Soluble Nanoparticle Catalysts. *Tetrahedron Lett.* **2017**, *58*, 82–86. (f) Shila, A. K.; Das, P. Solid Supported Platinum(0) Nanoparticles Catalyzed Chemoselective Reduction of Nitroarenes to *N*-Arylhydroxylamines. *Green Chem.* **2013**, *15*, 3421–3428. (g) Andreou, D.;

Iordanidou, D.; Tamiolakis, I.; Armatas, G. S.; Iykyakis, I. N. Reduction of Nitroarenes into Aryl Amines and *N*-Aryl Hydroxylamines via Activation of NaBH₄ and Ammonia-Borane Complexes by Ag/TiO₂ Catalyst. *Nanomaterials* **2016**, *6*, 54–66.

(33) (a) Karwa, S. L.; Rajadhyaksha, R. A. Selective Catalytic Hydrogenation of Nitrobenzene to Phenylhydroxylamine. *Ind. Eng. Chem. Soc.* **1987**, *26*, 1746–1750. (b) Takenaka, Y.; Kiyosu, T.; Choi, J. C.; Sakakura, T.; Yasuda, H. Selective Synthesis of *N*-aryl Hydroxylamines by the Hydrogenation of Nitroaromatics Using Supported Platinum Catalysts. *Green Chem.* **2009**, *11*, 1385–1390. (c) Rylander, P. N.; Karpenko, I. M.; Pond, G. R. Selectivity in Hydrogenation over Platinum Catalysts: Nitroaromatics. *Ann. N. Y. Acad. Sci.* **1970**, *172*, 266–275.

(34) Acharyya, S.; Ghosh, S.; Bal, R. Catalytic Oxidation of Aniline to Azoxybenzene Over CuCr₂O₄ Spinel Nanoparticle Catalyst. *ACS Sustainable Chem. Eng.* **2014**, *2*, 584–589.

(35) (a) Wheeler, O. H.; Gonzalez, D. Oxidation of Primary Aromatic Amines with Manganese Dioxide. *Tetrahedron* **1964**, *20*, 189–193. (b) Wenkert, E.; Wickberg, B. General Methods of Synthesis of Indole Alkaloids. A Flavopereirine Synthesis. *J. Am. Chem. Soc.* **1962**, *84*, 4914–4919. (c) Firoubabadi, H.; Mostafavipoor, Z. Barium Manganate. A Versatile Oxidant in Organic Synthesis. *Bull. Chem. Soc. Jpn.* **1983**, *56*, 914–917. (d) Ghosh, S.; Acharyya, S. S.; Sasaki, T.; Bal, R. Room temperature selective oxidation of aniline to azoxybenzene over a silver supported tungsten oxide nanostructured catalyst. *Green Chem.* **2015**, *7*, 1867–1876. (e) Baumgar, H. E.; Stalk, A.; Miller, E. M. Reactions of Amines. XIII. The Oxidation of *N*-Acyl-*N*-arylhydroxylamines with Lead Tetraacetate. *J. Org. Chem.* **1965**, *30*, 1203–1206.

(36) (a) Chang, C. F.; Liu, S. T. Catalytic Oxidation of Anilines into Azoxybenzenes on Mesoporous Silicas Containing Cobalt Oxide. *J. Mol. Cat. A: Chem.* **2009**, *299*, 121–126. (b) Cai,

S.; Rong, H.; Yu, H.; Liu, X.; Wang, D.; He, W.; Li, Y. Room Temperature Activation of Oxygen by Monodispersed Metal Nanoparticles: Oxidative Dehydrogenative Coupling of Anilines for Azobenzene Syntheses. *ACS Catal.* **2013**, *3*, 478–486.

(37) (a) Girrane, A.; Corma, A.; Garcia, H. Gold-Catalyzed Synthesis of Aromatic Azo Compounds from Anilines and Nitroaromatics. *Science* **2008**, *322*, 1661–1664. (b) Pahalagedara, M. N.; Pahalagedara, L. R.; He, J.; Miao, R.; Gottlieb, B.; Rathnayake, D.; Suib, S. L. Room Temperature Selective Reduction of Nitrobenzene to Azoxybenzene over Magnetically Separable Urchin-Like Ni/Graphene Nanocomposites. *J. Catal.* **2016**, *336*, 41–48. (c) Liu, Z.; Huang, Y.; Xiao, Q.; Zhu, H. Selective Reduction of Nitroaromatics to Azoxy Compounds on Supported Ag–Cu Alloy Nanoparticles Through Visible Light Irradiation. *Green Chem.* **2016**, *18*, 817–825. (d) Zhang, Z.-P.; Wang, X.-Y.; Yuan, K.; Zhu, W.; Zhang, T.; Wang, Y.-H.; Ke, J.; Zheng, X.-Y.; Yan, C.-H.; Zhang, Y.-W. Free-Standing Iridium and Rhodium-Based Hierarchically-Coiled Ultrathin Nanosheets for Highly Selective Reduction of Nitrobenzene to Azoxybenzene under Ambient Conditions. *Nanoscale* **2016**, *8*, 15744–15752.

(38) Montolio, S.; Vicent, C.; Aseyev, V.; Alfonso, I.; Burgette, M. I.; Tenhu, H.; García-Verdugo, E.; Luis, S. V. AuNP-Polymeric Ionic Liquid Composite Multicatalytic Nanoreactors for One-Pot Cascade Reactions. *ACS Catal.* **2016**, *6*, 7230–7237.

(39) Magiera, D.; Szmigielska, A.; Pietrusiewicz, K. M.; Duddeck, H. Secondary Phosphine Oxides: Tautomerism and Chiral Recognition Monitored by Multinuclear NMR Spectroscopy of their Rh₂[(R)-MTPA]₄ Adducts. *Chirality* **2004**, *16*, 57–64.

(40) González-Gálvez, D.; Nolis, P.; Philippot, K.; Chaudret, B.; Leeuwen, P. W. N. M. Phosphine-Stabilized Ruthenium Nanoparticles: The Effect of the Nature of the Ligand in Catalysis. *ACS. Catal.* **2012**, *2*, 317–321.

(41) (a) Kitagawa, H.; Kojima, N.; and Nakajima, T. Studies of Mixed-Valence States in Three-Dimensional Halogen-Bridged Gold Compounds, $\text{Cs}_2\text{AuIAuIII}\text{X}_6$, (X = Cl, Br or I). Part 2. X-Ray Photoelectron Spectroscopic Study. *J. Chem. Soc. Dalton Trans.* **1991**, *0*, 3121–3125. (b) Conte, M.; Davies, C. J.; Morgan, D. J.; Davies, T. E.; Elias, D. J.; Carley, A. F.; Johnston, P.; Hutchings, G. Aqua Regia Activated Au/C Catalysts for the Hydrochlorination of Acetylene. *J. Catal.* **2013**, *297*, 128–136. (c) Zhao, J.; Gu, S.; Xu, X.; Zhang, T.; Yu, Y.; Di, X.; NI, J.; Pan, Z.; Li, X. Supported Ionic Liquid Phase Stabilized Au(III) Catalyst for Acetylene Hydrochlorination. *Catal. Sci. Technol.* **2016**, *6*, 3263–3270 (d) Luza, L.; Rambor, C. P.; Gual, A.; Fernandes, J. A.; Eberhardt, D.; Dupont, J. Revealing Hydrogenation Reaction Pathways on Naked Gold Nanoparticles. *ACS Catal.* **2017**, *7*, 2791–2799. (e) Fong, Y.-Y.; Visser, B. R.; Gascooke, J. R.; Cowie, B. C. C.; Thomsen, L.; Metha, G. F.; Buntine, M. A.; Harris, H. H. Photoreduction Kinetics of Sodium Tetrachloroaurate under Synchrotron Soft X-ray Exposure. *Langmuir* **2011**, *27*, 8099–8104. (f) Lovelock, K. R. J.; Smith, E. F.; Deyko, A.; Villar-Garcia, I. J.; Licence, P.; Jones, R. G. Water Adsorption on a Liquid Surface. *Chem. Commun.* **2007**, 4866–4868.

(42) Haiss, W.; Nguyen, T. K.; Thanh, N. T. K.; Aveyard, J.; Fernig, D. G. Determination of Size and Concentration of Gold Nanoparticles from UV–Vis Spectra. *Anal. Chem.* **2007**, *79*, 4215–4221.

(44) Said-Mohamed, C.; Niskanen, J.; Lairez, D.; Tenhu, H.; Maioli, P.; Fatti, N. D.; Vallee, F.; Lee, L.-T. Polymer-Modulated Optical Properties of Gold Sols. *J. Phys. Chem. C* **2012**, *116*, 12660–12669.

(44) (a) McFarland, A. D.; Haynes, C. L.; Mirkin, C. A.; Van Duyne, R. P.; Godwin, H. A. Color My Nanoworld. *J. Chem. Educ.* **2004**, *81*, 544A–544B. (b) Shi, L.; Buhler, E.; Boue, F.; Carn, F. J. How Does the Size of Gold Nanoparticles Depend on Citrate to Gold Ratio in Turkevich Synthesis? Final answer to a debated question. *Coll. Int. Sci.* **2017**, *492*, 191–198. (c) Schulz, F.; Homolka, T.; Bastus, N. G.; Puentes, V.; Weller, H.; Vossmeier, T. Little Adjustments Significantly Improve the Turkevich Synthesis of Gold Nanoparticles. *Langmuir* **2014**, *30*, 10779–10784.

(45) (a) Li, J.; Shi, X.-Y.; Bi, Y.-Y.; Wei, J.-F.; Chen, Z.-G. Pd Nanoparticles in Ionic Liquid Brush: A Highly Active and Reusable Heterogeneous Catalytic Assembly for Solvent-Free or On-Water Hydrogenation of Nitroarene under Mild Conditions. *ACS Catal.* **2011**, *1*, 657–664. (b) Chatterjee, M.; Chatterjee, A.; Kawanami, H.; Ishizaka, T.; Suzuki, T.; Suzuki, A. Rapid Hydrogenation of Aromatic Nitro Compounds in Supercritical Carbon Dioxide: Mechanistic Implications via Experimental and Theoretical Investigations. *Adv. Synth. Catal.* **2012**, *354*, 2009–2018. (c) Verho, O.; Gustafson, K. P. J.; Nagendiran, A.; Tai, C.-W.; Bäckvall, J.-E. Mild and Selective Hydrogenation of Nitro Compounds using Palladium Nanoparticles Supported on Amino-Functionalized Mesocellular Foam. *ChemCatChem* **2014**, *6*, 3153–3159.

(46) (a) Roy, S.; Rao, A.; Devatha, G.; Pillai, P. P. Revealing the Role of Electrostatics in Gold-Nanoparticle-Catalyzed Reduction of Charged Substrates. *ACS Catal.* **2017**, *7*, 7141–7145. (b) Zhuang, Q.; Yang, Z.; Sobolev, Y. I.; Beker, W.; Kong, J.; Grzybowski, B. A. Control and

Switching of Charge-Selective Catalysis on Nanoparticles by Counterions. *ACS Catal.* **2018**, *8*, 7469–7474.